

# Performance-based earthquake engineering in a lower-seismicity region: South Korea

Han-Seon Lee\* and Ki-Hyun Jeong<sup>a</sup>

*School of Civil, Environmental and Architectural Engineering, Korea University, Seoul 02841, Korea*

*(Received December 20, 2017, Revised March 20, 2018, Accepted March 22, 2018)*

**Abstract.** Over the last three decades, Performance-based Earthquake Engineering (PBEE) has been mainly developed for high seismicity regions. Although information is abundant for PBEE throughout the world, the application of PBEE to lower-seismicity regions, such as those where the magnitude of the maximum considered earthquake (MCE) is less than 6.5, is not always straightforward because some portions of PBEE may not be appropriate for such regions due to geological differences between high- and low-seismicity regions. This paper presents a brief review of state-of-art PBEE methodologies and introduces the seismic hazard of lower-seismicity regions, including those of the Korean Peninsula, with their unique characteristics. With this seismic hazard, representative low-rise RC MRF structures and high-rise RC wall residential structures are evaluated using PBEE. Also, the range of the forces and deformations of the representative building structures under the design earthquake (DE) and the MCE of South Korea are presented. These reviews are used to propose some ideas to improve the practice of state-of-art PBEE in lower-seismicity regions.

**Keywords:** performance-based earthquake engineering; lower-seismicity regions; Korean Peninsula

## 1. Introduction

In many fields, conventional engineering design has been conducted to satisfy all of the engineering-code requirements. This design procedure is referred to as “design to prescriptive codes” in the present paper. The currently used prescriptive earthquake design codes are based on a traditional design philosophy to prevent the structural and nonstructural elements of buildings from being damaged in low-intensity earthquakes, limiting this damage to repairable levels during medium-intensity earthquakes, and preventing the overall or partial collapse of buildings in high-intensity earthquakes. After the 1994 Northridge and the 1995 Kobe earthquakes, the structural-engineering field realized that most of the damage, the economic loss that is due to downtime, and the structural repair costs are unacceptably high even though the corresponding structures complied with the current seismic codes based on the previously described traditional philosophy.

These realizations led to the development of the first-generation performance-based earthquake engineering (PBEE) guidelines of the U.S. Vision 2000 report (SEAOC 1995), for which the designation of the desired system performances at various seismic-hazard intensity levels was applied in the defining of the design framework of performance-based earthquake designs. A consultation occurs between the designer and the owner regarding the

selection of a desired combination of the performance and hazard levels that can be used as the design criteria. In the subsequent documents of the first-generation PBEE, such as the ATC 40 (1996), FEMA 273 (1996), FEMA 356 (2000), SEAONC (2007), Willford *et al.* (2008), ASCE 41-13 (2013), LATBSDC (2017), TBI (2017). The elemental deformation and the force-acceptability criteria that correspond to the performance are specified for different structural and non-structural elements with respect to linear, nonlinear, static, and dynamic analyses. These criteria do not contain probability distributions for both the demand and supply sides. Also, the elemental performance evaluation is not tied to the global performance.

Considering the shortcomings of the first-generation procedures that cannot be utilized for a probabilistic calculation of the system performance measures such as monetary loss, downtime, and casualties, which are expressed in terms of the direct interests of various stakeholders, the second-generation PBEE guidelines were developed by the Pacific Earthquake Engineering Research Center (PEER) in the U.S. The key feature of this methodology is a rigorous and probabilistic performance calculation. Accordingly, the uncertainty regarding the earthquake intensity, ground-motion characteristics, structural response, physical damage, and economic and human losses is explicitly considered in this approach.

The second-generation PBEE methodology like the PEER PBEE consists of the following four successive analyses: hazard, structural, damage, and loss. The performances of these analyses, however, have only occurred for regions with a strong seismicity such as the U.S. state of California. The present paper includes a brief review of the state-of-the-art PBEE methodologies. Then, the seismic hazard for regions with a lower seismicity

---

\*Corresponding author, Professor  
E-mail: [hslee@korea.ac.kr](mailto:hslee@korea.ac.kr)

<sup>a</sup>Ph.D. Student

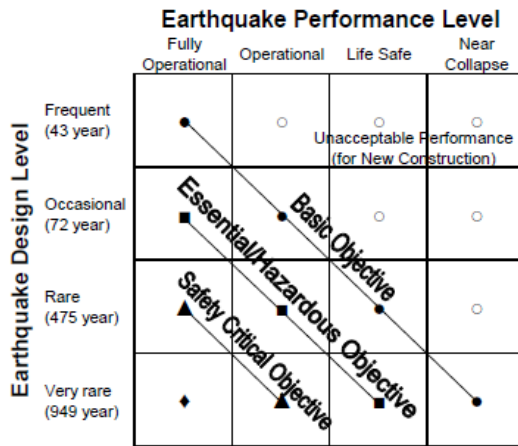


Fig. 1 Recommended seismic-performance objectives of the Vision 2000 report regarding buildings (SEAOC 1995)

including the Korean Peninsula is introduced with its unique characteristics. With this seismic hazard, representative low-rise reinforced concrete (RC) moment-resisting frame (MRF) structures and high-rise RC-wall residential structures are evaluated using PBEE approaches. Also, the ranges of the forces and the deformations of the representative building structures in South Korea are given. Based on these reviews and evaluations, a number of ideas regarding the improvement of the state-of-the-art PBEE practice in lower-seismicity regions are proposed.

## 2. History of PBEE

Section 2.1: Introduction excerpts from a part of the reference Porter (2003) and section 2.2: PEER PBEE from a part of the reference Moehle and Deierlein (2004).

### 2.1 Introduction

PBEE implies the design, evaluation, construction, and monitoring of the function and loads in response to the diverse needs and objectives of owners-users and society. It is based on the premise that performance can be predicted and evaluated with a quantifiable confidence to make intelligent and informed trade-offs together with the client, based on life-cycle considerations rather than solely the construction costs (Krawinkler and Miranda 2004).

PBEE in one form or another may supersede load-and-resistance-factor design (LRFD) as the framework under which many new and existing structures are analyzed for seismic adequacy. A key distinction between the two approaches is that LRFD seeks to assure performance primarily in terms of failure probability of individual structural components (with some system aspects considered, such as the strong-column-weak-beam requirement), whereas PBEE attempts to address performances primarily at the system level in terms of risk of collapse, fatalities, repair costs, and post-earthquake loss of function.

Initial efforts to frame and standardize PBEE methodologies produced SEAOC's Vision 2000 report

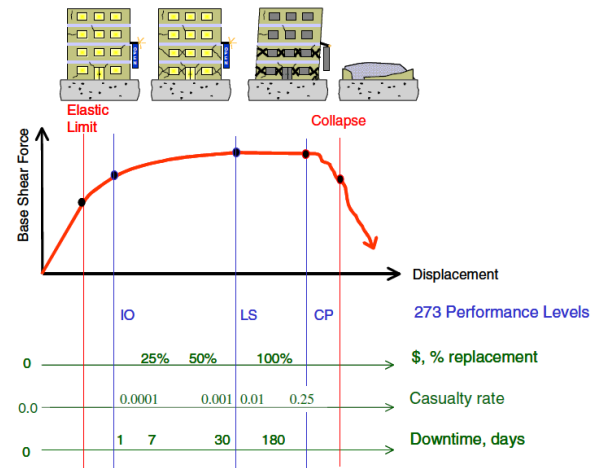


Fig. 2 Visualization of PBEE methodology (Moehle and Deierlein 2004)

(1995), FEMA 273 (1997), a product of the ATC-33 project. The authors of these documents frame PBEE as a methodology to assure combinations of desired system performance at various levels of seismic excitation. The system performance states of Vision 2000 include fully operational, operational, life safety, and near collapse. Levels of excitation include frequent (43-year return period), occasional (72-year), rare (475-year) and very rare (949-year) events. These reflect Poisson-arrival events with 50% exceedance probability in 30 years, 50% in 50 years, 10% in 50 years, and 10% in 100 years, respectively. The designer and owner consult to select an appropriate combination of performance and excitation levels to use as design criteria, such as those suggested in Fig. 1.

FEMA 273 expresses design objectives using a similar framework, although with slightly different performance descriptions and levels of seismic excitation. Each global performance level is detailed regarding the performance of individual elements. The design is believed to satisfy its global objectives if the structural analysis indicates that the member forces or deformations imposed on each element do not exceed predefined limits. Performance is binary and largely deterministic: if the member force or deformation does not exceed the limit, it passes; otherwise, it fails. If the acceptance criteria are met, the design is believed to assure the performance objective, although without a quantified probability. Other important pioneering PBEE efforts include ATC-32 (1996a), ATC-40 (1996b), and FEMA 356 (2000).

### 2.2 PEER PBEE

PBEE seeks to improve seismic risk decision-making through assessment and design methods that have a strong scientific basis and that express options in terms that enable stakeholders to make informed decisions. A key feature is the definition of performance metrics that are relevant to decision making for seismic risk mitigation. The methodology needs to be underpinned by a consistent procedure that characterizes the important seismic hazard and engineering aspects of the problem, and that relates

these quantitatively to the defined performance metrics. The first generation of PBEE assessment and design procedures for buildings in the United States made important steps toward the realization of PBEE. These procedures conceptualized the problem as shown in Fig. 2. Here, the building is visualized as being loaded by earthquake-induced lateral forces that result in nonlinear response and resulting damage. Relations are then established between structural response indices (interstory drifts, inelastic member deformations, and member forces) and performance-oriented descriptions such as Immediate Occupancy, Life Safety, and Collapse Prevention. Without minimizing the remarkable accomplishments of these first-generation procedures, several shortcomings can be identified:

- Engineering demands are based on simplified analysis techniques, including static and linear analysis methods; where dynamic or nonlinear methods are used, calibrations between calculated demands and component performance are largely lacking.
- The defined relations between engineering demands and component performance are based somewhat inconsistently on relations measured in laboratory tests, calculated by analytical models, or assumed on the basis of engineering judgment; consistent approaches based on relevant data are needed to produce reliable outcomes.
- Structural performance is defined by component performance states, where the overall system performance is assumed to be equal to the worst performance calculated for any component in the building.

Although the developers widely recognized the shortcomings of the first-generation procedures, limitations in available technologies and supporting research did not permit further development at that time. Since then, the PEER Center has embarked on a research program aimed at developing a more robust methodology for PBEE. Recognizing the complex, multi-disciplinary nature of the problem, PEER has broken the process into logical elements that can be studied and resolved in a rigorous and consistent manner. The process begins with a definition of a ground motion Intensity Measure ( $IM$ ), which defines in a probabilistic sense the salient features of the ground motion hazard that affect structural response. The next step is to determine Engineering Demand Parameters, which describe structural response regarding deformations, accelerations, or other response quantities calculated by simulation of the

building to the input ground motions. Engineering Demand Parameters are next related to Damage Measures, which describe the condition of the structure and its components. Finally, given a detailed probabilistic description of damage, the process culminates with calculations of Decision Variables, which translate the damage into quantities that enter into risk management decisions. Consistent with current understanding of the needs of decision-makers, the decision variables have been defined in terms of quantities such as repair costs, downtime, and casualty rates (Fig. 2). Underlying the methodology is a consistent framework for representing the inherent uncertainties in earthquake performance assessment.

While full realization of the methodology in professional practice is still years away, important advances are being made through research in PEER. Some specific highlights are presented in the following text.

Given the inherent uncertainty and variability in seismic response, it follows that a performance-based methodology should be formalized within a probabilistic basis. Referring to Fig. 3, PEER's probabilistic assessment framework is described in terms of four main analysis steps (hazard analysis, structural/nonstructural analysis, damage analysis, and loss analysis). The outcome of each step is mathematically characterized by one of four generalized variables: Intensity Measure ( $IM$ ), Engineering Demand Parameter ( $EDP$ ), Damage Measure ( $DM$ ), and Decision Variable ( $DV$ ). Recognizing the inherent uncertainties involved, these variables are expressed in a probabilistic sense as conditional probabilities of exceedance, i.e.,  $p[A|B]$ . Underlying the approach in Fig. 3 is the assumption that the performance assessment components can be treated as a discrete Markov process, where the conditional probabilities between parameters are independent.

The first assessment step entails a hazard analysis, through which one evaluates one or more ground motion  $IM$ . For standard earthquake intensity measures (such as peak ground acceleration or spectral acceleration)  $IM$  is obtained through conventional probabilistic seismic hazard analyses. Typically,  $IM$  is described as a mean annual probability of exceedance,  $p[IM]$ , which is specific to the location ( $O$ ) and design characteristics ( $D$ ) of the facility. The design characteristics might be described by the fundamental period of vibration, foundation type, simulation models, etc. In addition to determining  $IM$ , the hazard analysis involves characterization of appropriate ground motion input records for response history analyses.

Given  $IM$  and input ground motions, the next step is to

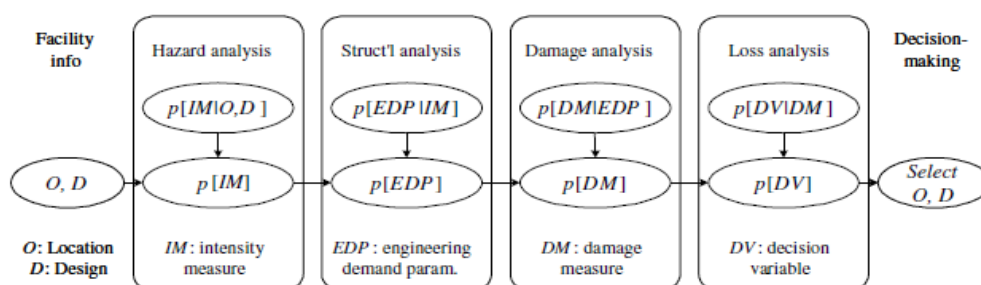


Fig. 3 The underlying probabilistic framework (Moehle and Deierlein 2004)

perform structural simulations to calculate *EDP*, which characterize the response in terms of deformations, accelerations, induced forces, or other appropriate quantities. For buildings, the most common *EDPs* are interstory drift ratios, inelastic component deformations and strains, and floor acceleration spectra. Relationships between *EDP* and *IM* are typically obtained through inelastic simulations, which rely on models and simulation tools in areas of structural engineering, geotechnical engineering, SSFI (soil-structure-foundation-interaction), and non-structural component and system response.

The next step in the process is to perform a damage analysis, which relates the *EDPs* to Damage Measures, *DM*, which in turn describes the physical damage to a facility. The *DMs* include descriptions of damage to structural elements, non-structural elements, and contents, in order to quantify the necessary repairs along with functional or life safety implications of the damage (e.g., falling hazards, the release of hazardous substances, etc.). These conditional probability relationships,  $p(DM|EDP)$ , can then be integrated with the *EDP* probability,  $p(EDP)$ , to give the mean annual probability of exceedance for the *DM*, i.e.,  $p(DM)$ .

The final step in the assessment is to calculate Decision Variables, *DV*, in terms that are meaningful for decision makers. Generally speaking, the *DVs* relate to one of the three decision metrics discussed above with regard to Fig. 2, i.e., direct dollar losses, downtime (or restoration time), and casualties. In a similar manner as done for the other variables, the *DVs* are determined by integrating the conditional probabilities of *DV* given *DM*,  $p(DV|DM)$ , with the mean annual *DM* probability of exceedance,  $p(DM)$ .

The methodology just described and shown in Fig. 3 is an effective integrating construct for both PBEE methodology itself and the PEER research program. The methodology can be expressed in terms of a triple integral based on the total probability theorem, as stated in Eq. (1).

$$v(DV) = \iiint G\langle DV|DM \rangle dG\langle DM|EDP \rangle dG\langle EDP|IM \rangle d\lambda(IM) \quad (1)$$

Though this equation form of the methodology might be construed as a minimalist representation of a very complex problem, it nonetheless serves a useful function by providing researchers with a clear illustration of where their discipline-specific contribution fits into the broader scheme of PBEE and how their research results need to be presented. The equation also emphasizes the inherent uncertainties in all phases of the problem and provides a consistent format for sharing and integrating data and models developed by researchers in the various disciplines.

The proposed methodology is intended to serve two related purposes. The first of these is as a performance engine to be applied in full detail to the seismic performance assessment of a facility. As illustrated in Fig. 2, the application would result in a comprehensive statement of the probabilities of various losses (in terms of dollars, downtime, and casualties) for events or time frames of interest to the owner or decision maker for that facility. Though illustrated in an apparent static loading domain in Fig. 2, this is for illustrative purposes only; the intent is to

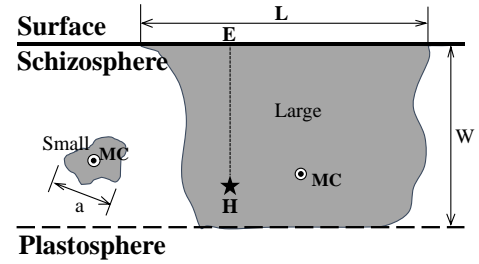


Fig. 4 Diagram illustrating the definitions of small and large earthquakes, showing the hypocenter (*H*), epicenter (*E*), moment centroid (*MC*), and the rupture dimensions of *a*, *L*, and *W* (Scholz 2002)

apply the methodology using a fully nonlinear dynamic analysis.

It leads to the second intended purpose of the methodology. Presuming it can be used to provide reliable results for a complete facility analysis, the methodology then can be used as a means of calibrating simplified procedures that might be used for the advancement of future building codes. It is in this application that the methodology is likely to have its largest potential impact.

### 3. Seismic hazard in South Korea

#### 3.1 Characteristics of the seismic hazard in the lower seismicity regions

Earthquakes can be divided into the following two classes: large earthquakes and small earthquakes. Small earthquakes are those events where the rupture dimensions are smaller than the width  $W^*$  of the schizosphere (Fig. 4). Therefore, this earthquake class propagates and terminates entirely within the bounds of the schizosphere, and their behaviors may be described as a rupture in an unbounded elastic-brittle solid. By contrast, a large earthquake is one in which a rupture dimension equals or exceeds the width of the schizosphere. Once an earthquake becomes large, it is constrained to only a horizontal propagation, with its aspect ratio increasing as it grows, while its top edge is at the free surface and its bottom is at the base of the schizosphere (Scholz 2002).

Although approximately 95% of the global seismic-moment release is produced by plate-boundary earthquakes, major distances separate significant numbers of earthquakes from the plate boundaries. These intraplate earthquakes are important because they greatly expand the region of the possible seismic hazard from the proximity of the plate boundaries. Their role in tectonics is poorly understood, both from the viewpoint of the origin of the forces that generate them and the types of structures that localize them. One way that a distinction can be made between interplate and intraplate earthquakes is based on the slip rate of their faults and therefore their recurrence time, as explained in Table 1. Intraplate earthquakes are classified into two types. The Type II earthquakes occur in broad zones near the plate boundaries that they are tectonically related to, or they occur in diffuse plate boundaries. Examples are the

Table 1 Classification of tectonic earthquakes (Scholz 2002)

Type	Slip rate ( $v$ ), mm/yr.	Recurrence time, yrs.
I. Interplate	$v > 10$	$\sim 100$
II. Intraplate, plate boundary related	$0.1 \leq v \leq 10$	$10^2 \sim 10^4$
III. Intraplate, midplate	$v < 0.1$	$> 10^4$

earthquakes of the Basin and Range provinces of western North America (WNA), which, in a very broad sense, may be considered as a part of the Pacific-North America plate boundary or the inland earthquakes of Japan, the latter of which is tectonically a part of the compressional Pacific-Eurasian plate margin. In contrast, Type III earthquakes occur in midplate regions and seem to be unrelated to the plate boundaries. This classification is of course somewhat artificial, because there is a continuous spectrum of earthquake types and slip rates. An important reason for this classification, however, is the distinct difference between the source parameters of the so-defined intraplate and interplate earthquakes, and the corresponding systematic stress drops are higher by a factor of three compared with those of the interplate earthquakes (Scholz 2002).

It is known that either very infrequent major earthquakes or infrequent moderate earthquakes have occurred in eastern North America (ENA). In either case, the more recent seismic activity is minor. An example might be a region with a single recorded occurrence of an earthquake with a magnitude of 7 or larger, and without a damaging earthquake in the time since (e.g., Memphis, Charleston, or Boston), or a string of earthquakes of a magnitude from 5 to 5.5 and sufficient geologic evidence to imply the possibility of a rare larger event. The localities are not expectant, nor are they generally prepared for an earthquake, and for the most part, the buildings are not earthquake-resistant. Typically, these regions are located away from the tectonic-plate boundaries and major faults, leading to a less-comprehensive and more difficult understanding of the source of the earthquakes, while the hazard assessments are more difficult. Further, the earthquake-caused ground shaking diminishes, or “attenuates,” to a much lesser degree as the distance from the earthquake increases. This finding means that, for a given magnitude, the “felt area” and the extent of damage are much greater in most of the moderate seismic regions compared with the high seismic regions (Nordenson and Bell, 2000). A number of active faults have been identified, where the average historic slip rate is 1 mm per year or more, in the seismic-activity evidence of the Holocene times (the past 11000 years), while all of the faults are hidden faults (FEMA 450).

The shaking effects of the Charleston, South Carolina, earthquake on August 31, 1886, indicate that it is a major shock. The moment-magnitude estimates range from an  $M_w$  of 6.9 to 7.3 (Chapman *et al.* 2016). Notably, this earthquake is an exceptionally large-magnitude earthquake where a surface rupture did not occur; therefore, an important piece of direct field evidence, the direction of the fault-surface trend, which is termed by geologists as the

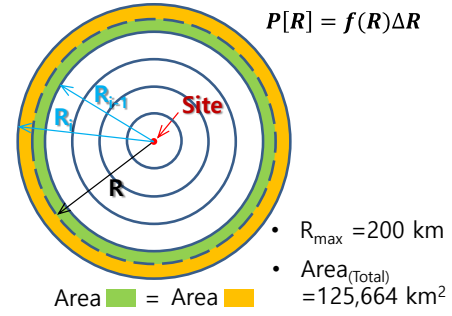


Fig. 5 Probability of the occurrence of an earthquake assuming the uniform distribution of the seismicity for a background earthquake (Lam *et al.* 2016)

*strike*, was not provided for this earthquake, and nor was the fault-movement direction and whether it is vertical, horizontal, or a combination (Nuttli *et al.* 1986).

### 3.2 Background seismic hazard in South Korea that determines the minimum earthquake load

The Probabilistic Seismic Hazard Analysis (PSHA) is composed of four steps. The first step is the identification of all of the earthquake sources. Secondly, the relation between the magnitude of the earthquake and its frequencies needs to be statistically represented according to the Gutenberg-Richter recurrence law. The third is the establishment of the attenuation law between the ground-motion parameters and the rupture or epicentral distance where the median and the standard deviation of the ground-motion parameters are to be obtained. Lastly, the fourth step is the derivation of the hazard curve that is represented by the relation between the hazard parameter and the exceedance probability of the specific parameter value.

For a uniform background zone, it is assumed that the probability of the occurrence of an earthquake (Fig. 5) is uniform throughout a region, so the occurrences for each earthquake level are distributed uniformly, as shown in Table 2.

The earthquake-recurrence relationship of Fig. 6, under the assumption of a doubly-truncated exponential function, can be expressed as follows

$$\lambda_M = v \frac{\exp[-\beta(M - M_{min})] - \exp[-\beta(M_{max} - M_{min})]}{1 - \exp[-\beta(M_{max} - M_{min})]}$$

$$M_{min} \leq M \leq M_{max}, M_{min} = 4$$

$$v = \exp(\alpha - \beta M_{min}) = 10^{(a - bM_{min})}$$

$$\alpha = 2.3a$$

$$\beta = 2.3b$$
(3)

where  $\lambda_M$  is the number of earthquakes with a magnitude greater than  $M$  that occur in a fixed time interval and within the circular source area of the radius  $R_{max}$ ;  $v$  is the total number of earthquakes with a magnitude greater than  $M_{min}$ , which occur in a fixed time interval and within the circular source area;  $\beta = 2.3b$ , in which  $b$  is the slope of the Gutenberg-Richter relationship, and in this approach,  $b = 0.9$  is used; the mean yearly number of the earthquakes with a magnitude that is greater than or equal to the  $M_{min}$ , which is assumed to be 4, is represented by  $10^a$ ; and the  $a$  value of 3.03 was derived

Table 2 Number of  $M \geq 5$  intraplate earthquake events on land in a 50 years period (Lam *et al.* 2016)

Country	Land Area (km)	$N(M \geq 5)$ in 50 years (Recorded Number)	$N(M \geq 5)$ in 50 years (Recorded Number Normalized to 1,000,000 km <sup>2</sup> )
Australia	7,692,024	45	6
Brazil	8,515,767	33	4
Eastern US	2,291,043	13	5 – 6
Eastern & Central China	1,550,974	14	9
France	674,843	4	6
Southern India	635,780	3	5
Germany	357,021	1	3
British Isles	315,134	3	9 – 10
Peninsular Malaysia	131,598	<1	<1
Korean Peninsula	223,348	3	13
Total	$\Sigma = 22,387,532$	$\Sigma = 120$	Average = 5

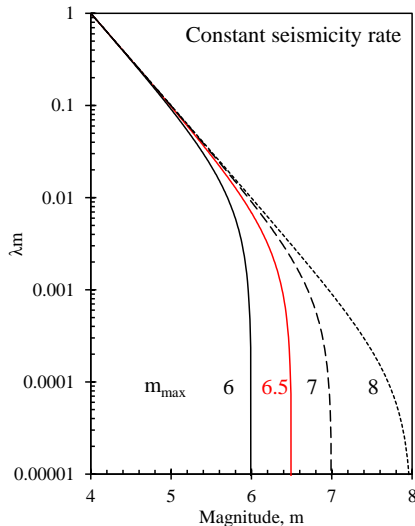


Fig. 6 Earthquake recurrence relationship

according to the number of earthquakes of  $M > 5$  that occurred in the last 50 years on the Korean Peninsula, as given in Table 2.

The corresponding probability density function (PDF) is defined as follows

$$f(M) = \frac{\beta \exp[-\beta(M - M_{min})]}{1 - \exp[-\beta(M_{max} - M_{min})]} \quad (3)$$

In Fig. 7, the assumed probability distribution of the peak horizontal acceleration (PHA) in South Korea is the same as that given by the ground-motion prediction equation (GMPE) of Boore (2008). For each combination of the epicentral distance, magnitude, and PGA, the exceedance probability ( $PGA \geq y^*$ ) can be obtained using Eq. (4), as follows

$$P[PGA > y^* | m, r] = 1 - F_Y \left( \frac{\ln y^* / \ln PGA}{\sigma_{\ln PGA}} \right) \quad (4)$$

where  $m$  is the moment magnitude;  $r$  is the epicentral distance;  $y$  is the acceleration of the ground motion determined by the  $m$ -

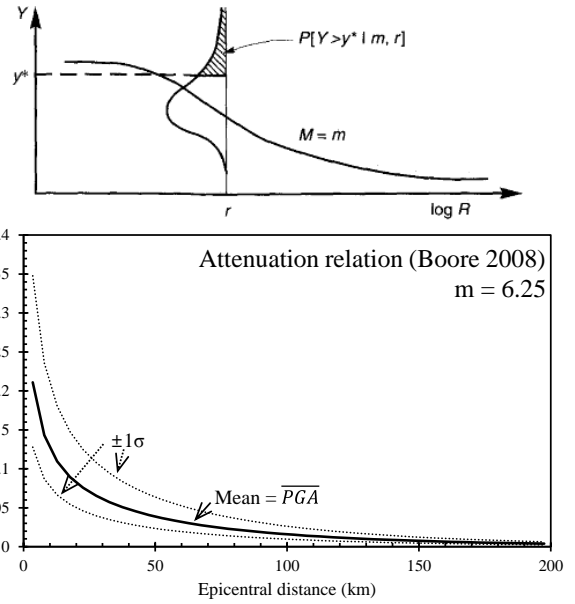


Fig. 7 Relationship between the epicentral distance and the peak ground acceleration (PGA)

Table 3 Comparison between the Effective Peak Ground Acceleration (PGA) of the Korean Building Code (KBC) 2016 and the Background Hazards

Return periods (year)	KBC 2016	Background Hazard
500	0.11g	0.025g
2500	0.22g	0.054g

$r$  combination;  $F_Y$  is the value of the CDF of  $y$ ;  $\sigma_{\ln PGA}$  is the standard deviation of the natural logarithm of the PGA.

For every combination of  $m$  and  $r$  here, the seismic intensities are predicted through the employment of suitable GMPEs. Lastly, the total seismic hazard of the site that encompasses all of the considered  $m$ - $r$  combinations can be computed using the conventional Cornell-McGuire approach (Cornell 1968, McGuire 1976) that is represented by the following integral

$$\lambda_{y^*} = \nu \sum_{j=1}^{N_M} \sum_{k=1}^{N_R} P[Y > y^* | m_j, r_k] P[m_j] P[r_k] \quad (5)$$

The exceedance probability, or the annual frequency of the  $PGA \geq y^*$ , are based on the uniform background zone for which the Table 2 data for the Korean Peninsula and the GMPE (Boore, 2008) are shown in Fig. 8, and the PGAs that correspond to the exceedance probabilities of 10% and 2% over 50 years are 0.025 g and 0.054 g, respectively. The value of 0.025 g for the probability of 10% in 50 years is similar to the value of 2.5% in the uniform background zone in the ENA (Frankel, 1995). These PGAs are compared with the effective PGAs in the Korean Building Code (KBC) 2016 (Table 3), wherein the PGAs are approximately four times larger than those that are based on the uniform background zone of the Korean Peninsula.

The disaggregation for a PGA of 0.054 g (Fig. 9) is shown in the histograms on the epicentral distance and the magnitude. This figure shows that most of the contribution comes from

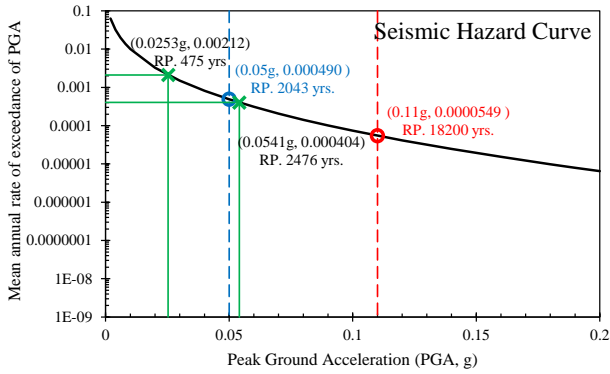


Fig. 8 Mean annual rate of the exceedance of the peak ground acceleration (PGA) for the Korean Peninsula

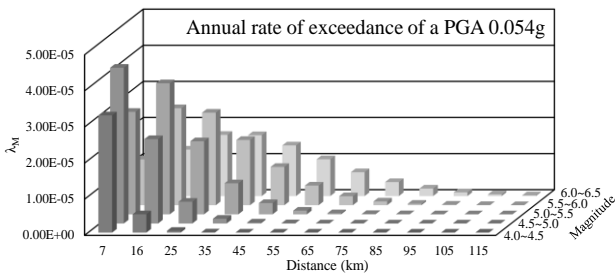


Fig. 9 Disaggregation for PGA of 0.054 g

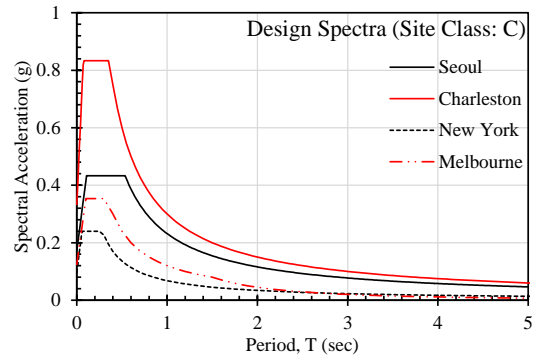
within a distance that is less than 50 km and from magnitudes ranging from M 4.0 to 6.5. In the lower-seismicity regions such as the ENA and the Korean Peninsula, the hazard that is derived from the uniform background zone serves as the lower bound for the probabilistic seismic-hazard map.

### 3.3 Seismic loads in lower-seismicity regions

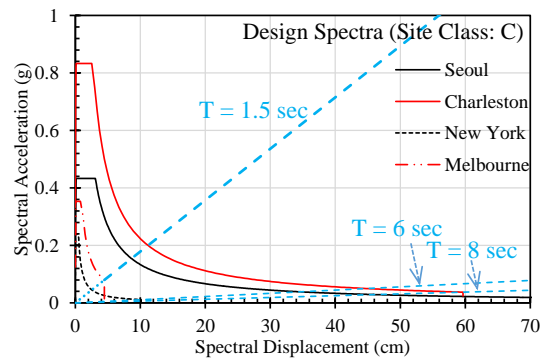
#### 3.3.1 Comparison of the seismic loads in lower-seismicity regions

The ENA is one of the representative moderate-seismicity regions in the world, and a methodology was very competently developed for higher seismicity regions in WNA in terms of the seismic-hazard analysis. Two representative cities of the ENA are New York City and Charleston, which experienced a strong earthquake in 1886. The earthquake-load pseudo spectral accelerations (PSAs) on Site: C for these two cities in the International Building Code (IBC) and the American Society of Civil Engineers (ASCE) 7 at the short period (0.2 s) and 1 s are  $S_S=0.3$  g and  $S_1=0.06$  g for New York City, and  $S_S=1.25$  g and  $S_1=0.3$  g for Charleston, respectively (Fig. 10). The corner period between the velocity-constant and displacement-constant regions are 6 s and 8 s for New York City and Charleston, respectively.

The Australian continent is a representative intraplate region. Australia developed its seismic-hazard map and the seismic load based on an analysis of its historical and instrumental earthquake records. Fig. 10 also shows a comparison of the design spectra in Melbourne, Australia, and that in Seoul, South Korea, corresponding to the soil condition C. The Australia spectrum comprises two corner periods, where the second corner period,  $T_2$ , determines the displacement-constant region. The value of  $T_2$  in Australia is



(a) Design spectra



(b) Acceleration-displacement response spectra (ADRS)

Fig. 10 Design spectra for Seoul (Korean Building Code (KBC)), Charleston (American Society of Civil Engineers (ASCE)), New York (ASCE), and Melbourne (Australian/New Zealand Standard (AS/NZS))

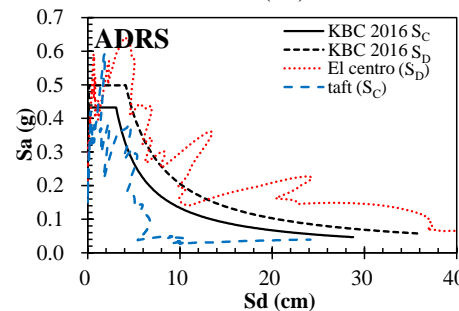
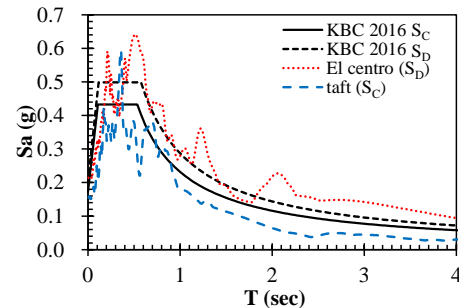


Fig. 11 Comparison among KBC2016, El Centro, and Taft Spectra

1.5 s, which is much smaller than the 6 s and the 8 s of New York City and Charleston, respectively. Also, it can be seen that the acceleration-displacement response spectra (ADRS) of the South Korean design spectrum is much larger than that of Melbourne.



(a) Special details of shear walls



(b) Mock-up test of special shear wall (30-story residential building in Daegu, Korea)

Fig. 12 Construction problems with special details required for SDC D (Chung *et al.*, 2013)

Table 4 Seismic Design Categories with the SDS, SD1 determined for site conditions in KBC compared with those in IBC

Site Class	KBC 2016		IBC 2000		IBC 2006 (New York)		Seismic Design Category (SDC)			
	$S_{DS}^*$ (g)	$S_{D1}^*$ (g)	Sacramento, CA, SDC II	$S_{DS}$ (g)	$S_{D1}$ (g)	Seismic Design Category (SDC)				
	Special I II		IV III I, II							
$S_A$	0.293	0.117	C	B	B	0.160	0.032	A	A	A
$S_B$	0.366	0.146	D	C	C	0.200	0.040	B	B	C
$S_C$	0.439	0.234	D	D	D (C)	0.240	0.068	B	B	C
$S_D$	0.527	0.336	D	D	D	0.312	0.096	B	B	C
$S_E$	0.732	0.497	D	D	D	0.468	0.140	D	C	C

### 3.3.2 Seismic-load and design requirement of South Korea

The current KBC design spectra are shown in Fig. 11, and they are compared with the response spectra of the 1940 El Centro earthquake ( $M_W=6.9$ ) and the 1952 Taft earthquake ( $M_W=7.3$ ). These figures clearly reveal that the Korean earthquake design loads are not actually for lower earthquake ground motions, but are for those that are genuinely strong.

The level of the earthquake load for each risk category of the building structures determines the seismic design category (SDC), as shown in Table 4. The zone factor of 0.22 g in Seoul has the SDC D for the soil conditions  $S_C$ ,  $S_D$ , and  $S_E$ , where SDC D means that the seismic details (for a strong-seismicity region) can be imposed with other additional requirements. The situation in Seoul is similar to the case of Sacramento in California, U.S., as shown in Table 4; however, New York City in the ENA comprises only one D for the soil condition,  $S_E$ , and the highest risk category of IV.

Table 5 Design factors for RC lateral force-resisting systems (Fardis 2014)

Code	Seismic Force-Resisting System	KBC 2016					IBC 2006 (=ASCE 7-10)				
		Design factors		Height limit			Design factors		Height limit		
		$R$	$\Omega_0$	$C_d$	C	D	$R$	$\Omega_0$	$C_d$	C	D
Bearing wall systems	Special RC walls	5	2.5	5	-	-	5	2.5	5	-	50m
	Ordinary RC walls	4	2.5	4	-	60m	4	2.5	4	-	X
Building frame systems	Special RC walls	6	2.5	5	-	-	6	2.5	5	-	50m
	Ordinary RC walls	5	2.5	4.5	-	60m	5	2.5	4.5	-	X
Moment resisting frame (MRF)	Special MRF	8	3	5.5	-	-	8	3	5.5	-	-
	Intermediate MRF	5	3	4.5	-	-	5	3	4.5	-	-
	Ordinary MRF	3	3	2.5	-	X	3	3	2.5	X	X
Dual systems with special MRF	Special RC walls	7	2.5	5.5	-	-	7	2.5	5.5	-	-
	Ordinary RC walls	6	2.5	5	-	-	6	2.5	5	-	X
Dual systems with intermediate MRF	Special RC walls	6.5	2.5	5	-	-	6.5	2.5	5	-	50m
	Ordinary RC walls	5.5	2.5	4.5	-	60m	5.5	2.5	4.5	-	X

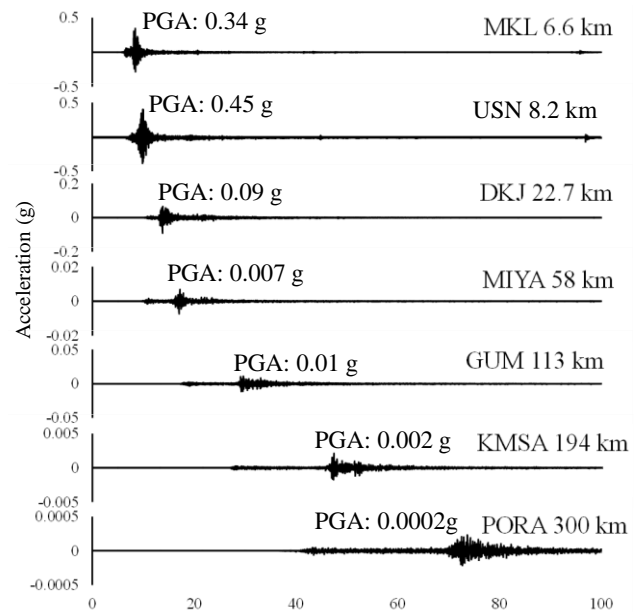


Fig. 13 EW component of Gyeongju earthquake records

The classified lateral force-resisting building system of Table 5 contains a number of differences between the KBC 2016 and the IBC 2006. The height limit for high-rise building structures is one example, as the KBC 2016 requires special seismic details for building structures of a height that exceeds 60 m and that belong to the design category D. Most of the residential buildings in Korea do not belong to this category, but more of the recently constructed residential buildings exceed this height limit, and they have consequently become subject to special detailing requirements, as shown in Fig. 12,



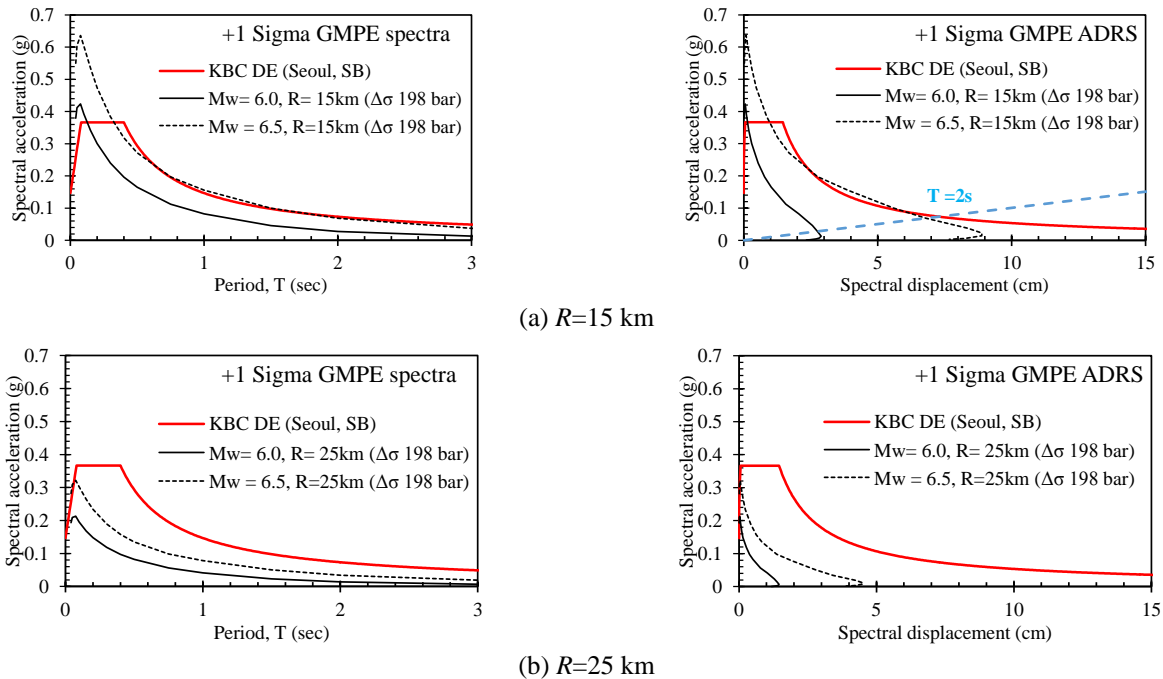
(a) Failure of column at the base of structure (KBS)

(b) Shear failure of short columns (Lee 2017)



(c) Damages of non-structural element (roof tile, window, goods) (YTN, Ohmynews)

Fig. 14 Damage and failure modes during 2016 Gyeongju Earthquake



(a)  $R=15$  km

(b)  $R=25$  km

Fig. 15 Comparison of the GMPE, where  $\Delta\sigma=198$  bar and the response spectra are based on South Korean earthquake records with the KBC design spectrum (Jeong and Lee 2018)

where the reinforcement congestion that is due to this requirement causes construction difficulties.

### 3.4 Implications of recent earthquakes in South Korea

A moderate-sized earthquake of a local magnitude  $M_L$  of 5.8 occurred on September 12, 2016. The events including the foreshock and the aftershock occurred around the Yangsan fault zone in the south-eastern Korean Peninsula that had been

seismically inactive. This earthquake is the largest event in the Korean Peninsula since 1978 when the national seismic monitoring began. The PGAs reached 0.45 g in the east-west (E-W) component, 0.43 g in the north-south (N-S) component, and 0.23 g in the vertical component at the USN station at an epicentral distance of 8.2 km (Fig. 13). The spectra of the displacement waveforms at local stations (MKL and USN) displayed characteristic high-frequency energy values. The responsible fault rupture was not found on the surface. For

detailed information on this earthquake, refer to Hong *et al.* (2017).

A brittle- shear failure occurred at the short columns in the basement of a five-story residential-building structure and under the roof of a temple, as shown in Figs. 14(a) and 14(b). Many nonstructural failures occurred such as the falling of oriental-roof tiles, window-glass breakages, and the falling of store objects, as shown in Fig. 14(c).

Fig. 15 compares the PSAs obtained from mean +1 sigma values of the developed GMPE ( $\Delta\sigma=198$  bar) that were developed by Jeong and Lee (2018) based on the records of the recent 11 earthquakes whose  $M_L>4$  including the Gyeongju earthquake ( $M_L=5.8, M_W=5.4$ ) with the design spectrum of the KBC 2016. The soil condition assumed in this GMPE and that of the design spectrum are the  $S_B$  ( $V_{S,30}=760$  m/s~1500 m/s). The PSAs of the GMPE with the  $M_W$  of 6.5 -  $R_{HYPO}$  of 15 km are 1.5 times larger than the design spectrum of the KBC at a period of 0.1 s, but similar to values of PSA at the periods beyond 0.4 s. The spectral displacements (SD's) of the GMPE at periods longer than 2 s do not exceed 8 cm. The PSAs and the SDs of the GMPE with an  $M_W$  of 6.5- $R_{HYPO}$  of 15 km generally match to design spectrum of the KBC 2016. Refer to Jeong and Lee (2018) for the details of the derivation of this GMPE.

The PSA of the GMPE at a short period of 0.1 s decreased by half with the increase of the hypocentral distance from 15 to 25 km, thereby showing a rapid decay of the high frequency. The PSAs of the GMPE with an  $M_W$  of 6.5- $R_{HYPO}$  of 25 are much lower than those of the KBC.

While the short-period PSAs with an  $M_W$  of 6.0 are approximately 70% of those with an  $M_W$  of 6.5, the long-period SDs of an  $M_W$  of 6.0 are only approximately 40% of those of the  $M_W$  of 6.5. This finding means that a long-period SD is more sensitive to the magnitude. Therefore, building structures that are designed according to the KBC guidelines seem to be capable of sustaining the ground motion with an  $M_W$  of 6.5 and with a hypocentral distance that is beyond approximately 15 km. That is, the PSA at an epicentral distance of 25 km does not represent damage to the structure has been designed and constructed according to the current seismic code.

The design spectrum of the building codes is based on qualitative evaluations of PSHA (Atkinson 2004, Lam *et al.* 2016). Although this comparison of the design spectrum with those of the GMPE developed herein intends to identify the characteristic of the scenario earthquake in a lower-seismicity region such as South Korea, it does not mean that the current design spectrum should be modified accordingly. To develop a design spectrum compatible with the Korean Peninsula, more systematic research using probabilistic seismic hazard analysis is necessary in the future.

#### 4. PBEE in a lower-seismicity region: South Korea

##### 4.1 PBEE for an RC MRF that is designed with different levels of the earthquake load in South Korea

The evaluation of a typical low-story RC MRF building structure in Seoul, South Korea, was performed using PBEE. The prototype is shown in Fig. 16 (effective ground-motion

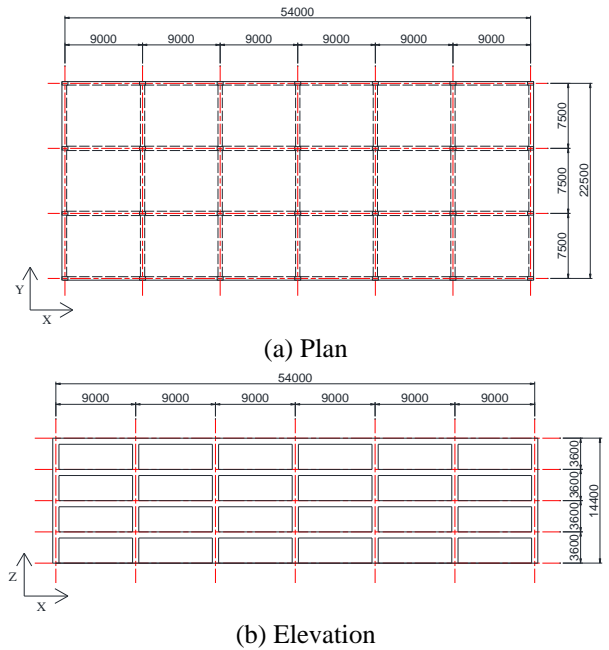


Fig. 16 Prototypical building structure: four-story reinforced concrete (RC) moment-resisting frame (MRF) in South Korea

Table 6 Design seismic load of 4-story prototype building model according to KBC 2016

Parameter	Value	
	[ Design I ]	[ Design II ]
Seismic load	Earthquake with return period of 500 years	Design spectrum (KBC)
Seismic zone factor	$S = 0.11$ for Seoul	$S = 0.22$ for Seoul
Soil type	$S_C$	
Design spectral accelerations at 0.2s and 1.0s	$S_{DS}=0.330$ g; and $S_{D1}=0.174$ g	$S_{DS}=0.433$ g; and $S_{D1}=0.232$ g
Seismic design category	C	D
Response modification factor	$R=3$	
Displacement amplification factor	$C_d=2.5$	
Importance factor	$I_E=1.0$	
Fundamental period (empirical equation)	$T_a=0.540$ s	
Seismic coefficient ( $C_s=S_{D1}/(R/I_E \times 1.5T)$ )	$C_s = 0.1100$	$C_s = 0.1431$

factor,  $S=0.22$  g), wherein the floor area and the total area are 1215 m<sup>2</sup> and 4860 m<sup>2</sup>, respectively. The space is used as an office in South Korea and the Risk Category is "ordinary," or the Seismic Grade II, while the soil condition is represented by the  $S_C$ . This prototype was designed for two seismic-load levels, as follows: one corresponding to two-thirds of the intensity of the MCE with a return period of 2500 years, specified as KBC 2016, and the other corresponding to the intensity of the earthquake with a return period of 500 years. The details for these two load cases are shown in Table 6.

Fig. 17 shows the results of a unidirectional pushover analysis in the X and Y directions for these two designs. The

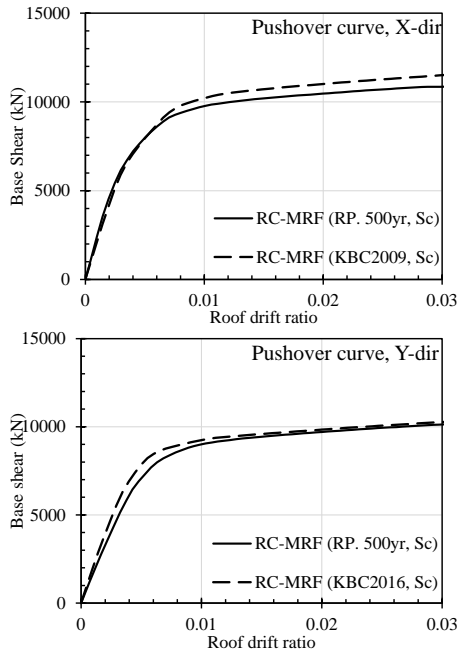


Fig. 17 Pushover curves in the X and Y directions

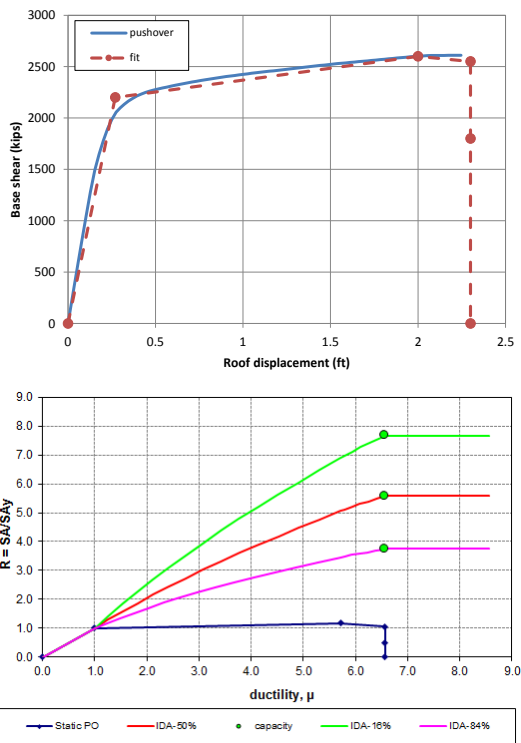


Fig. 18 Illustration of SPO2IDA for prototype buildings

fragility of the collapse was developed using the static pushover to incremental dynamic analysis (SPO2IDA) tool that is provided in the FEMA P58 (2012). Fig. 18 presents the bilinear model that is used in pushover analyses and the SPO2IDA concept regarding the collapse probability that is related to the results of the incremental dynamic analysis (IDA).

The collapse-fragility curves can be obtained by using the IDA results in the SPO2IDA, as shown in Fig. 19, where the value of the abscissa,  $S_a$ , represents the spectral acceleration at

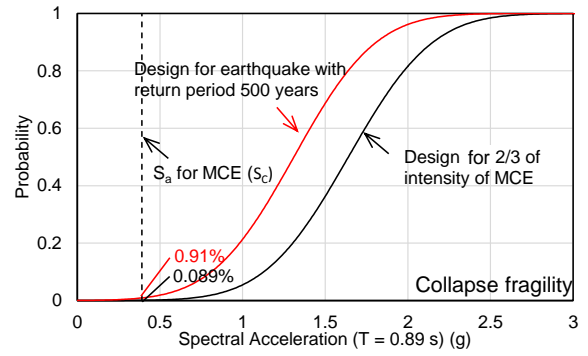


Fig. 19 Fragility curves of the prototype collapse

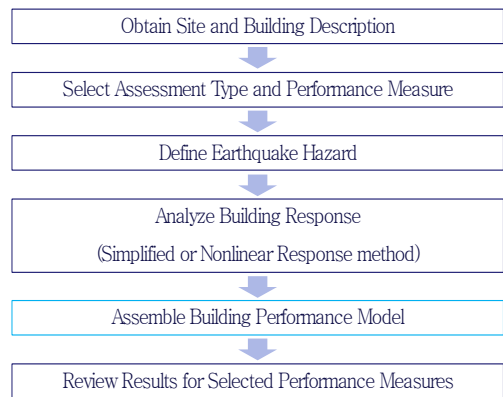


Fig. 20 Procedure for the loss estimation (FEMA-P58 2012)

the fundamental period of the prototype,  $T=0.89$  s. According to these collapse-fragility for MCE that are represented by  $S_a=0.39$  g ( $S_c$ ), Design I for the intensity of the earthquake with the return period of 500 years, the probability of collapse is 0.916%, while the intensity of two-thirds of the earthquake with the return period of 2500 years regarding Design II reveals a probability of 0.089%.

When the developed collapse fragility is the input into the Performance Assessment Calculation Tool (PACT) that is provided by the FEMA P58, the economic loss is predicted through the procedure of Fig. 20. The three options of the assessment type that are provided in the FEMA P58 are the Intensity, Scenario, and Time-based assessments. In this study, the Intensity assessment was used. The building response was analyzed using a simplified method such as SPO2IDA. The building-performance model and the results from this model are provided in the PACT. Table 7 shows the input items of the structural and nonstructural elements of the prototype.

In Table 8, the results of the economic loss and casualties are compared for the two designs with respect to the two seismic hazards that are represented by the earthquakes with the return periods of 500 and 2500 years. The seismic loads of Designs I and II are defined as the earthquake with the return period of 500 years in South Korea and that of two-thirds of the MCE intensity, respectively. It is assumed that the cost of the new construction will be US\$8 million with US\$1=₩1100, which is based on the average known cost of ₩6 million for 3.3 m<sup>2</sup> in Korea. When the building was subjected to the earthquake with a return period of 500 years, the repair costs were estimated as less than 10 % of the cost of the new construction, with the repair time being five months and the

Table 7 Input items of structural and nonstructural elements for the prototype (FEMA-P58 2012)

	Component Type	Quantity (unit) / story		Demand Parameter
		X dir.	Y dir.	
Column and beam joint	ACI 318 SMF, Concrete Column and beam =24"×24", beam both sides	28 (EA)	28 (EA)	IDR
Window	Curtain walls - Generic midrise stick-built curtain wall, config: monolithic, lamination: unknown, glass type: unknown, details: aspect ratio=6:5, other details unknown	69.73 (SF 30)	29.03 (SF 30)	IDR
Stair	Non-monolithic precast concrete stair assembly with concrete stringers and treads with no seismic joint.	2 (EA)	2 (EA)	IDR
Ceiling	Suspended ceiling, SDC A, B, Area (A): 1000<A<2500, vert support only	7.27 (SF 1800)		Floor Acceleration
Wall partition	Wall partition, type: gypsum with metal studs, full height, fixed below, fixed above	2.36 (LF 100)	2.70 (LF 100)	IDR

Table 8 Economic loss and casualties for the prototype

Return period (RP) of the target seismic load	Seismic design	Economic loss, billion ₩ (cost ratio: repair/rebuilding)	Repair time (day)	Casualties (peopl)
500 yrs. (10% exceedance in 50 yrs.)	Design I	0.82 (9%)	150	0.079
	Design II	0.38 (4%)	71	0.067
2500 yrs. (2% exceedance in 50 yrs.)	Design I	4.8 (55%)	360	0.955
	Design II	2.41 (28%)	339	0.725

Table 9 Seismic design load of 15-story prototype building according to KBC 2016

Parameter	Value
Seismic zone factor	$S = 0.176$ for Seoul
Soil type	$S_C$
Design spectral accelerations at 0.2s and 1.0s	$S_{D5}=0.352$ g; and $S_{D1}=0.191$ g
Seismic design category	C
Response modification factor	$R=4$
Displacement amplification factor	$C_d=4$
Importance factor	$I_E=1.2$
Fundamental period (empirical equation)	$T_{a,X-dir.}=1.17$ s; and $T_{a,Y-dir.}=0.787$ s
Seismic coefficient ( $C_s=S_{D1}/(R/I_E \times 1.5T)$ )	$C_{s,X-dir.}=0.0326$ ; and $C_{s,Y-dir.}=0.0485$
Effective seismic weight, $W$	$W=32,400$ kN
Design base shear ( $V=C_sW$ )	$V_{X-dir.}=1,060$ kN; and $V_{Y-dir.}=1,570$ kN

casualty rate being negligible. When the building was subjected to the earthquake with the return period of 2500 years, the number of casualties is still less than 1, but the repair costs for both Designs I and II increased to 55 and 28 % of the new-construction cost, respectively, with the repair time being almost one year. This means that even though the structure would not collapse, a relatively high repair cost and time may render a new construction.

4.2 PBEE for High-rise RC wall structure in South Korea

Several approaches for PBEE are proposed by SEAONC (2007), Willford *et al.* (2008), ASCE 41-13 (2013), LATBSDC (2017) and TBI (2017) to design or evaluate the seismic resistance of tall building structures. The PBEE approach proposed by FEMA-P58 is adopted to evaluate the seismic performance of the high-rise RC wall structure.

In South Korea, a major portion of the residential buildings (more than 60 % of the total residential units) has been constructed using RC-wall structures with the most typical height of 15 stories, as shown in Fig. 21. The most common plan of residential units that is the prototype of this study is a two-unit plan with a 15-story height, which is given in Fig. 22. The seismic design was conducted using the KBC2016, and the details are given in Table 9.

The seismic fragility of the prototype was obtained using the cloud method, as given by the Structural Engineers Association of California, Applied Technology Council, and California Universities for Research in Earthquake Engineering (SAC)/Federal Emergency Management Agency

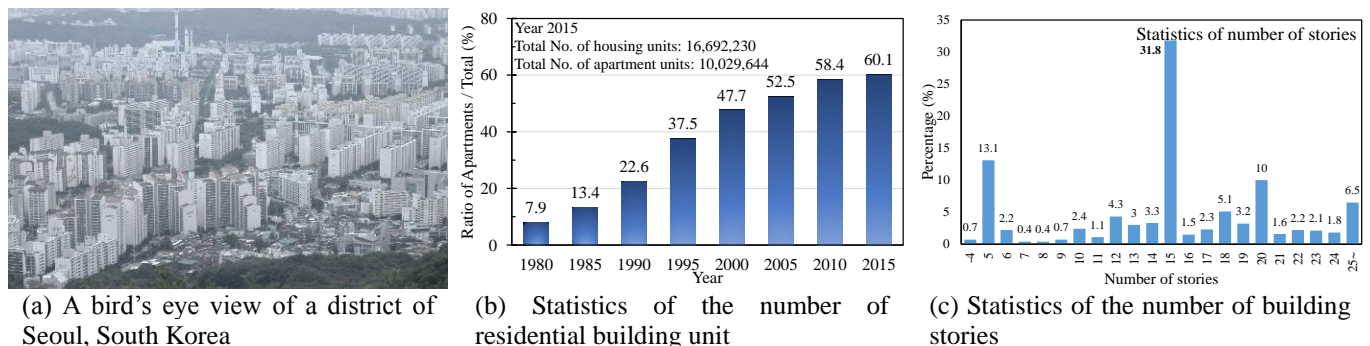


Fig. 21 High-rise RC residential building structures in South Korea

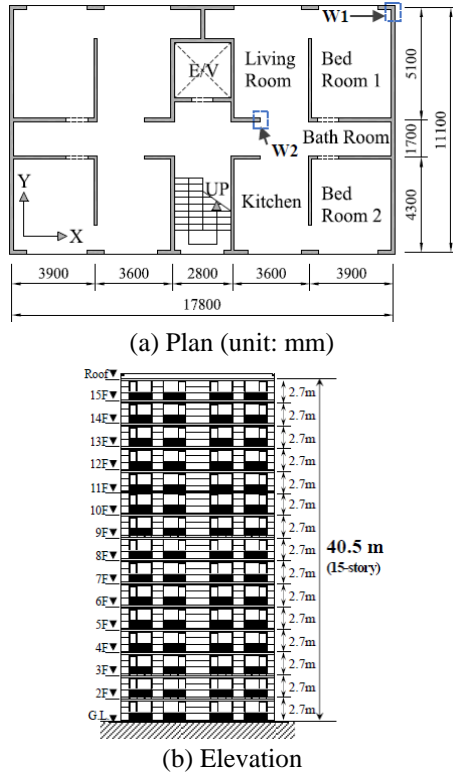


Fig. 22 Prototype building: 15-story RC wall building structure

Table 10 Definition of limit states, LS (Ji *et al.* 2007)

Level	Limit state (LS)	Description	IDR (%)
LS 1	Serviceability	Minor (including distributed) cracking in the primary load resisting structural system (crack width > 0.2 mm)	0.20
LS 2	Damage control	First yielding of longitudinal steel reinforcement; or presence of first plastic hinge	0.58
LS 3	Collapse prevention	Ultimate capacity of main load-resisting structural system; or point of decreasing capacity in overall load-deformation response	1.5

Table 11 Probability of exceeding LS1 to 3 under design earthquake (DE) and maximum considered earthquake (MCE) in South Korea

Limit state	DE		MCE	
	SAC/FEMA	IDA	SAC/FEMA	IDA
LS 1	79%	57%	97%	87%
LS 2	0.3%	1.7%	5.1%	10%
LS 3	0.00000358%	0.0000173%	0.000157%	0.000362%

(FEMA) approach (Cornell *et al.* 2000) and the IDA (FEMA-350, 2000). The fragility curves corresponding to the limit states (LSs) are described in Table 10 with their IDRs (%) and are shown in Fig. 23.

The probabilities of failure regarding each LS when the prototype was subjected to the DE and the MCE in South Korea are given in Table 11. The prototype has the probability

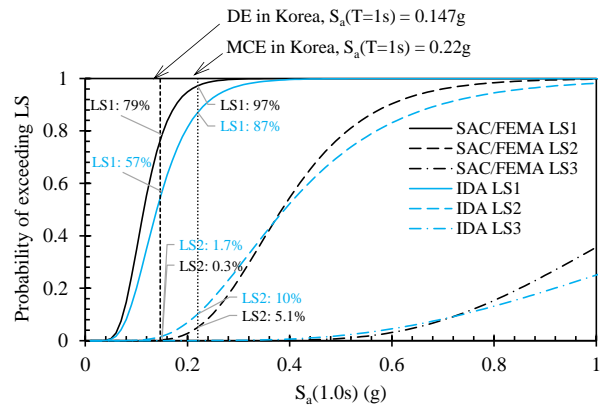


Fig. 23 Seismic fragility curves of a 15-story RC wall building structure

of 90% for the LS 1, which means the occurrence of major cracks (width > 0.2 mm) with that of the first yielding of the main reinforcement being approximately 10% under the MCE. However, the probability of the collapse of the 15-story RC-wall building structure appears to be very low not only for the DE but also for the MCE.

The seismic loss estimation was conducted using these fragility curves and the PACT, the tool that is provided by the FEMA P58. In this case, the Analyze Building Response in the procedure (Fig. 20) was conducted by using the Nonlinear Response Method instead of the Simplified Method. Then, the fragility of the RC-wall panel and the loss function regarding the repair cost and time that are implicit in the PACT were used. The resultant loss estimations are given in Figs. 24 and 25, where the economic loss of the prototype is estimated to be from US\$0.9 million to 3.7 million (median=1.8 million), while the repair time ranges from 75 to 300 days (median = 150 days) for the MCE.

### 5. Expected ranges of the force and the deformation in the building structures of South Korea

Research including earthquake simulations and pushover tests has been conducted (1) to identify seismic weaknesses in non-seismic RC building structures that have been designed only for gravity loads and (2) to observe the seismic performance of RC residential-building structures that have been designed per the recent South Korean seismic code. (Lee and Woo 2002a, Lee and Woo 2002b, Hwang and Lee 2015, Lee *et al.* 2015) From this research results, the expected ranges of the force and the deformation are summarized for PBEE in the lower-seismicity regions.

#### 5.1 1:5-scale RC 3-story ordinary MRF with nonseismic detailing

The objectives of the research of Lee and Woo (2002a) are the investigation of the seismic performance of an RC three-story ordinary MRF that has not been engineered to resist earthquake excitations. The prototype of this test model was adopted from a police-office building structure that was actually built and is in use in South Korea. The important

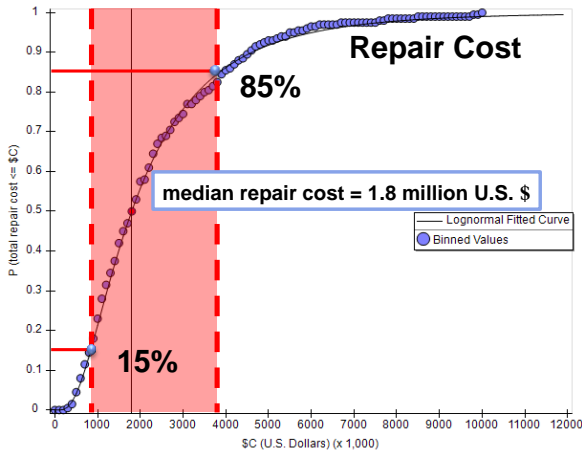


Fig. 24 Economic loss by the repair cost as given by PACT

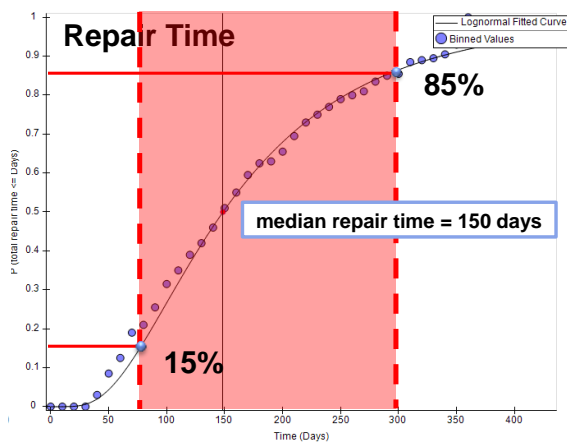


Fig. 25 Repair time as given by PACT

Table 12 Test program of the bare frame (BF) model

Identification of Test	PGA (g)	Remarks (Return Period)
Earthquake Simulation Test	TFT_012	0.12 Design earthquake (EQ.) in Korea (500 years)
	TFT_02	0.2 Max. EQ. in Korea (1000 years)
	TFT_03	0.3 Max. considered EQ in Korea (2000 years)
	TFT_04	0.4 Severe EQ. in high seismic regions of the world
Pushover Static Test	PUSH	- Ultimate capacity of the structure

characteristics of the Korean detailing practice are as follows: (1) The splice is located at the bottom of the column, (2) the spacing of the hoops is relatively large, (3) seismic hooks are not used, (4) confinement reinforcements are not used in the beam-column joints, and (5) the joints are composed of a special anchorage style.

This model was subjected to the shaking-table motions that simulate the earthquake ground motions of the Taft N21E component, whose PGA-magnitude values were modified to approximately 0.12, 0.2, 0.3, and 0.4 g in Table 12. Due to the limitation of the capacity of the used shaking table, a pushover test was performed to observe the ultimate structural capacity after the earthquake-simulation tests.

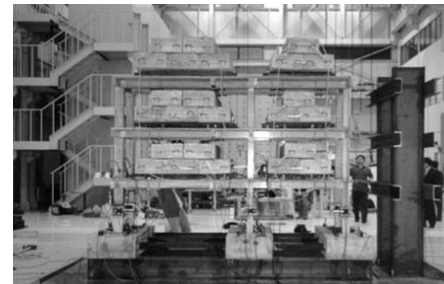
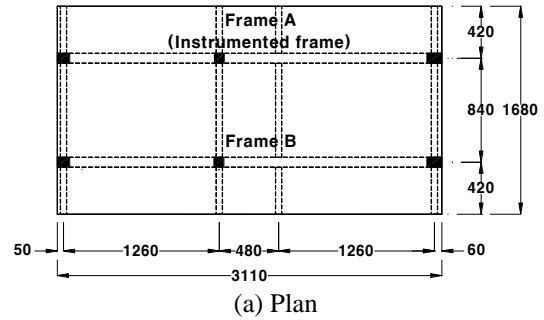
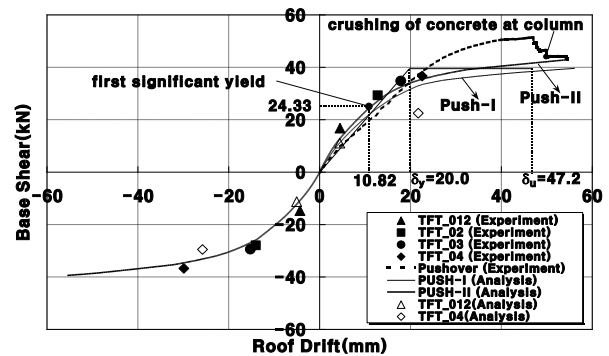
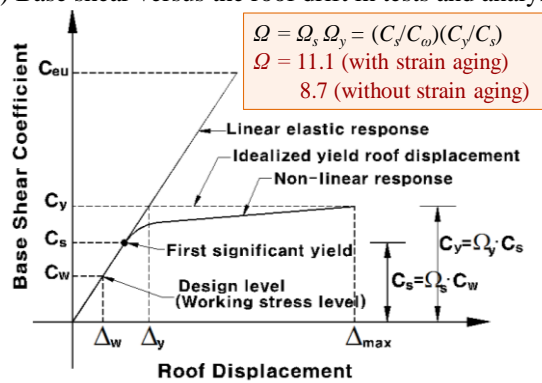


Fig. 26 1:5-scale 3-story RC moment-resisting frame model (Lee and Woo 2002a)



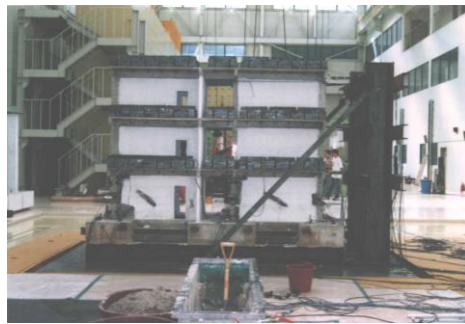
(a) Base shear versus the roof drift in tests and analyses



(b) Typical global structural response idealized as linearly elastic-perfectly plastic curve

Fig. 27 Test results of the BF model (Lee and Woo 2002a)

Although the bare frame (BF) model structure of this study (Fig. 26) was designed only for the gravity loads in lower-seismicity zones, the model showed a linear elastic behavior under the Taft N21E motion with the PGA of 0.12 g that represents a South Korean DE, and this can be seen in Fig. 27(a).



(a) Shaking table test of FIF



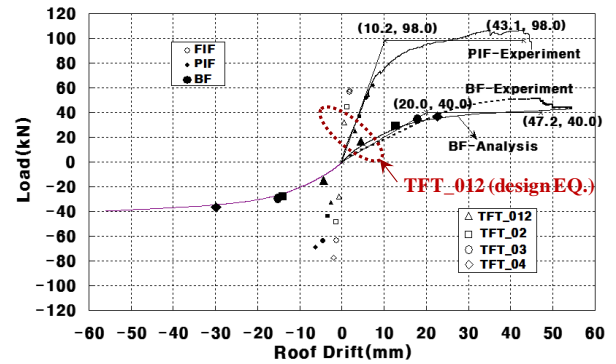
(b) Pushover test of PIF

Fig. 28 1:5-scale 3-story masonry-infilled RC frame model (Lee and Woo 2002b)

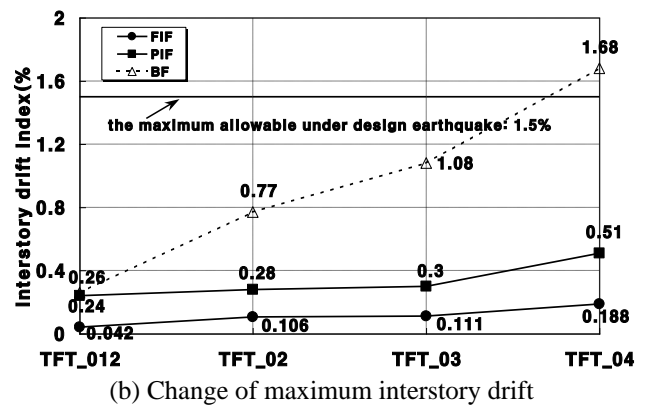
The structure could resist not only the DE, which it would be supposed to resist if it is designed to provide protection against earthquakes, but also the higher earthquake-excitation levels. The main component of its resistance to high-level earthquakes is a high over-strength, as shown in Fig. 27(b). The model structure demonstrated an overall displacement-ductility ratio of 2.4 and an overstrength factor of approximately 8.7.

### 5.2 1:5-scale 3-story masonry-infilled RC frame with nonseismic detailing

Lee and Woo (2002b) investigated the actual responses of a masonry-infilled RC frame with nonseismic detailing under the simulated-earthquake ground motions. After the earthquake-simulation tests, the monotonically-increasing lateral-load test or the pushover test was performed to determine the ultimate model capacities. By comparing these test results with those of the bare frame (Lee and Woo 2002a), the significance or the effect of the masonry infills was evaluated. The following two masonry-infill layouts were used for the earthquake-simulation tests, as shown in Fig. 28: fully infilled frame (FIF) and partially infilled frame (PIF). The adopted input ground accelerogram is the Taft N21E component, and as can be seen in Table 12, the modified PGA values are 0.12, 0.2, 0.3, and 0.4, which are the same as those of the BF model. After the series of earthquake-simulation tests were conducted using the FIF model, only minor cracks appeared in the masonry infills with the frame itself remaining intact for the PIF model. Therefore, a portion of the masonry infills was removed, as shown in Fig. 28(b), and then this PIF model was again subjected to the same series of earthquake-simulation tests as the FIF.



(a) Base shear versus the roof drift in tests



(b) Change of maximum interstory drift

Fig. 29 1:5-scale 3-story masonry-infilled RC frame model (Lee and Woo 2002b)

The masonry infills can be beneficial to the seismic performance of the structure since the amount of the strength increase appears to be twice as great as that of the induced-earthquake inertia forces, while the deformation capacity of the global structure remains almost the same regardless of the presence of the masonry infills. The maximum base-shear values of the FIF, PIF, and BF under the TFT\_012 DE test of South Korea are 32.0 kN, 37.3 kN, and 17.6 kN, respectively, which are shown in Fig. 29(a). These are from 2.5 to 5.3 times as much as the design base shear of 7.03 kN that is according to the South Korean seismic code. In Fig. 29(b), the maximum interstory drift indices (IDI) in the FIF and PIF models under the varying peak-input accelerations are shown, and the drifts of both the FIF and PIF models are significantly reduced compared to those of the BF. The PIF drifts are much greater than those of the FIF under the same level of the input ground motions. The IDI of neither the FIF nor the PIF, however, exceeds the maximum value of 1.5% that is allowed in the Korean seismic code, even under TFT\_04.

### 5.3 1:5-scale 10-story RC Box-type wall building structure model

The number of apartment housing units is more than 60% of the total number of housing units in Korea. These residential apartment buildings generally consist of high-rise reinforced concrete (RC) wall structures and, according to Korea Building Code (AIK 2005), should be designed and constructed to resist the earthquake while existing buildings not satisfying these codes should be evaluated and retrofitted. The seismic

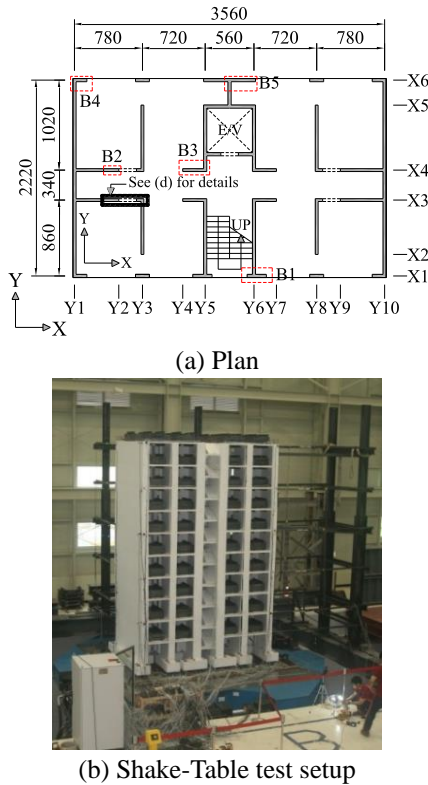


Fig. 30 1:5-scale 10-story RC box-type wall building structure model (Lee *et al*o 2012)

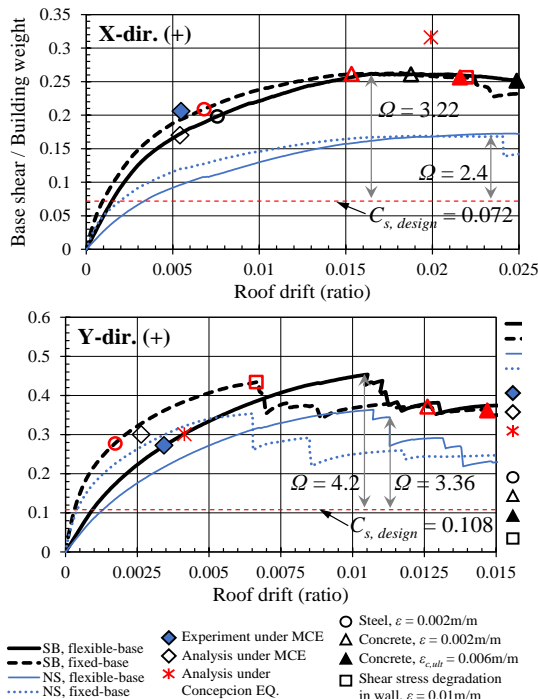


Fig. 31 Capacity curves of 1:5-scale 10-story RC box-type wall building structure model (Lee *et al.* 2012, Hwang and Lee 2015)

performance of the high-rise residential building model was evaluated based on the results of earthquake simulation tests (Lee *et al.* 2012) and nonlinear time history analyses (Hwang and Lee 2015).

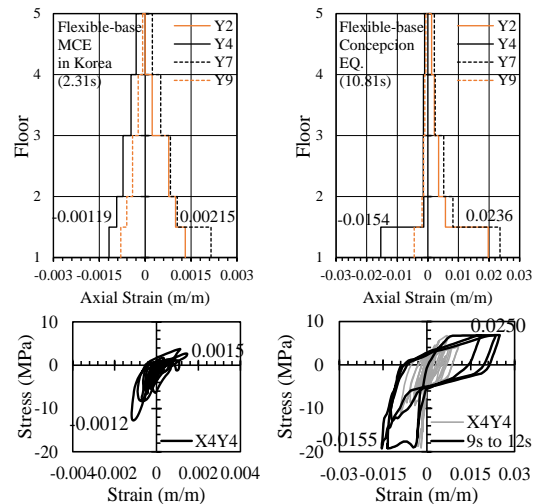


Fig. 32 Distribution of plastic hinges and axial strain of inner walls under MCE and Concepcion earthquake (Lee *et al.* 2012, Hwang and Lee 2015)

The prototype for the experiment was chosen to represent the most typical design in South Korea, and it was designed according to the old design code of the Architectural Institute of Korea (AIK), AIK2000 (AIK 2000). The thickness of the walls is 180 or 160 mm, while that of the slabs is 200 mm. The reinforcement of the walls is two contains, and the vertical-reinforcement ratio of the steel is in the range from 0.34 to 0.90 %, while the horizontal steel ratio is 0.29%. Considering the capacity of the available shaking table and the feasibility of the model reinforcements, a 10-story building model of the 1:5 scale was chosen (Fig. 30). To investigate the influence of the slab, the analytical model without the slabs was also modeled. The SB model consists of both slabs and coupling beams, while the NS model comprises only coupling beams without any slabs.

The experimental and analytical models possess a large overstrength (Fig. 31). Under the MCE in South Korea, the maximum base-shear coefficients of the experiment and the analysis are 0.206 and 0.17 in the X direction, respectively, and 0.272 and 0.30 in the Y direction, respectively, which are from 2.5-3.0 times larger than the seismic design coefficients,  $C_s$ , respectively, and 0.5 and 0.3 % roof drifts occurred in the X and Y directions, respectively. In the results of the static pushover analyses, the overstrength of the model with the slabs,  $\Omega$ , which is defined as the maximum strength ratio of the fully-yielded system to the seismic coefficient, is 3.22 in the X direction and 4.2 in the Y direction. The strength and deformation under the MCE in South Korea are only just exceeding the whole-structure yields. In the capacity curves, the lateral strength dropped suddenly after the peak-resistance point due to the shear failure in the Y-directional outer walls. The overstrength of the model is larger than the value of the overstrength factor of 2.5 that is given in the KBC 2005 and the IBC 2000.

In the test results, numerous horizontal cracks appeared in the outer walls at the lower stories that were subjected to a large membrane force. In the analytical model, the axial strains of the wall boundaries at various locations were calculated. Under the MCE in South Korea, the maximum axial-strain



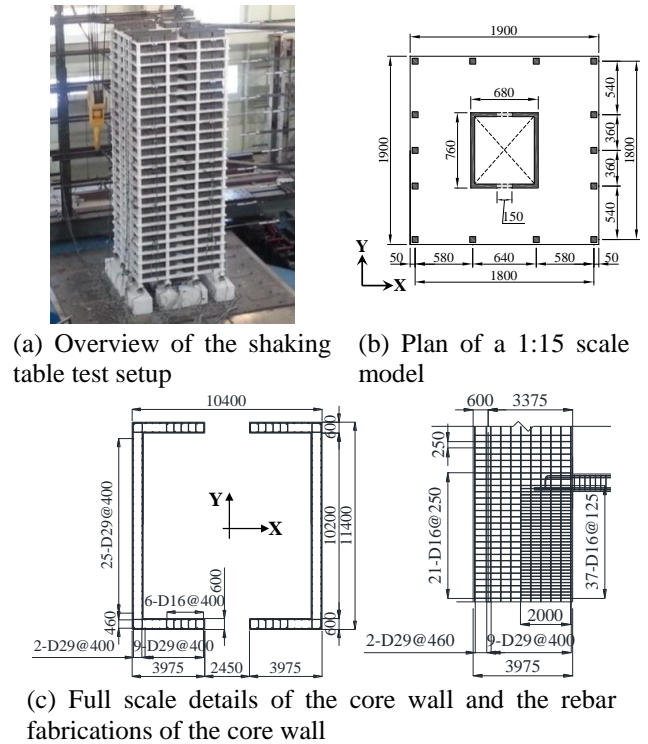
Fig. 33 Collapse of 10-story RC shear wall building in Chile earthquake (M 8.8, 2010, Concepcion) (ATC-92 2012)

demands of the wall boundaries in the lower part of the first story are within a tension of 0.006 m/m and a compression of 0.0012 m/m (Fig. 32). The tensile strains in the outer walls are larger than the value of the steel-yield strain of 0.002 m/m, which are consistent with the horizontal cracks of the experiment. The probability of the damage that is due to concrete crushing and rebar buckling is very low under the MCE in South Korea.

To investigate the seismic performance of the RC box-type-wall building during the 2010 Concepcion earthquake of Chile ( $M_w=8.8$ ), a nonlinear time-history analysis was conducted. Under this earthquake, the total dissipated energy is approximately 10 times larger than that under the MCE of South Korea. The maximum tensile and compressive strains of 0.0252 and 0.0154 m/m, respectively, occurred at the wall boundaries, thereby indicating a high potential for severe damage due to the concrete spalling, buckling, and fracture of the reinforcements at the walls that actually occurred during the 2010 Concepcion earthquake, as can be seen in Fig. 33.

#### 5.4 1:15-scale 25-story RC Flat-Plate Core-Wall building model

Recently, the number of high-rise buildings (higher than 30 stories) has been increasing in the interest of the efficient use of available housing sites. For these high-rise buildings, a combined system of core shear walls is utilized, as follows: a lateral load-resistance structural system and flat plates have been extensively used along with a gravity-load-resisting structural system. These structural types in the current seismic provisions of the KBC 2009 and the IBC 2006 are classified as a dual-frame or building-frame system. For the shear walls in the building-frame system, special shear walls, for which special seismic-detailing requirements are imposed, or the ordinary shear walls that are limited by a height restriction, have generally been used. In both the dual-frame and building-frame systems, two vertical shear walls often include regular openings and are connected to each other with coupling beams that exert a considerable effect on the lateral-resistance behavior. The most typical type of the RC-flat-plate core-wall building structure was chosen for the prototype that was originally a 35-story flat-plate building in which each floor contained four dwelling units. However, due to the limitations of the shaking-table capacity, the number of stories in the prototype for the shaking-table test was reduced to 25 and the



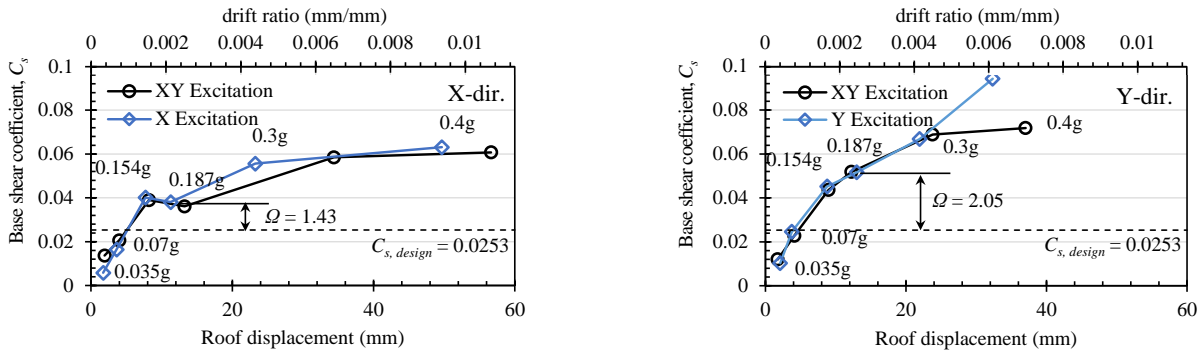
(d) Details of the core wall and the rebar fabrications of the core wall of the 1:15 scale model

Fig. 34 1:15-scale 25-story RC flat-plate core-wall building model (Lee *et al.* 2015)

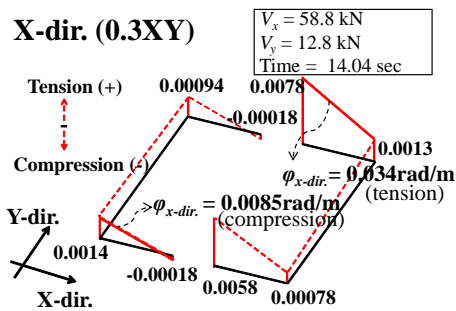
model was scaled down to 1:15, as shown in Figs. 34(a) and 34(b). Figs. 34(c) and 34(d) show the special-wall details of the prototype and the model. The overview of shaking table tests on 1:15 scale 25-story RC flat-plate core-wall building model plan, and the details are then given in Fig. 34.

In Fig. 35(a), under the design earthquake in Korea (DE, 0.187XY), the base-shear coefficients are 0.0361 in the X direction and 0.0518 in the Y direction, and these are 1.5- and 2-times larger than the designed base-shear coefficient of 0.0253, respectively.

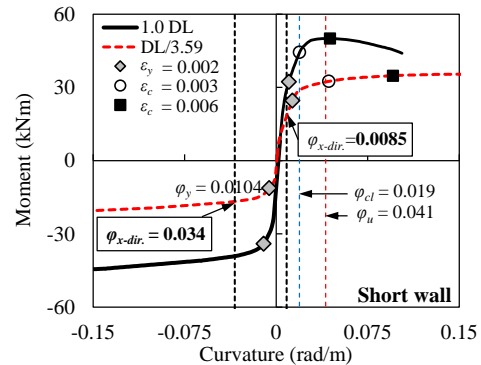
In accordance with the displacement-based design method that is proposed in the ACI 318-05, special boundary details were imposed on the short wall in the first story with the expected plastic rotation of  $\theta_p=0.00537$  rad, which is shown in Fig. 35(b). No significant plastic deformation was observed under the MCE in South Korea. At the bottom 70 mm of the first story, the measured maximum curvature when the end of the boundary element in the short wall is under compression is  $\phi_{x-dir}=0.0085$  rad/m, which is approximately 21% of 0.041 rad/m, the ultimate corresponding curvature in relation to the



(a) Correlation between the maximum roof drift and the base shear coefficient



(b) Strain distribution of the core wall at the bottom of the first story under MCE

(c) Relation between the moment and the curvature (M- $\phi$ ) in the core wall (X-dir.)Fig. 35 Shake-table test results of a 1:15-scale 25-story RC flat-plate core-wall building model (Lee *et al.* 2015)

expected compressive strain of 0.00638 m/m, as shown in Fig. 35(c). This result implies that the design requirements on the boundary elements of the walls that are given in ACI 318-05 could be overly conservative, particularly for the wall design of high-rise RC building frames or dual-frame structures with more than 20 stories.

## 6. Summary and conclusions

### 6.1 Summary

The characteristics of the earthquake ground motions in lower seismicity regions are as follows:

- The collapse probability can be very low in lower-seismicity regions, whereas the probability of nonstructural damage is very high. Losses from the nonstructural-component damage can be a major portion of the economic loss.
- The damage can be concentrated in the region within a short epicentral distance.
- The duration is relatively short, so the resonance effect can be minor, and the intensity of the high-frequency contents is very high at the near field, but it decays very rapidly as the epicentral distance is increased.
- Spectral high-frequency accelerations are very high and can cause brittle failures such as the shear failure of the short columns and the crushing of the window glasses.
- The spectral displacement can be significantly small when compared with the spectral acceleration; therefore,

the probability of flexible structures being involved in large inelastic excursions is generally low.

- The impact of high-frequency ground motions on the lower-frequency structures can cause a nonvibratory unidirectional overload to the shear-critical members such as short columns.
- Typical building structures in a lower seismicity region such as South Korea, which were not designed seismically, have retained a large overstrength, so it is not reasonable to assume all the non-seismically designed building structures would collapse as many media rouse the public to the unjustified fear.
- Generally, the deformation range that is expected in South Korea does not cause severe damage, and it is not necessary to adopt special details; this can lead to the alleviation of the ductile-detail requirement.

The success of PBEE in high-seismicity regions as well as lower-seismicity regions depends on the way that actual behavior and loss are reasonably estimated. That is, every assumption of the analysis should be verified with an observation of realistic structural behaviors. An estimation of the earthquake load should be ascertained by the real records of the earthquake ground motions, and the rationale for the extrapolation of the ground-motion prediction equation to the maximum-magnitude earthquake should be provided. The following prerequisites are required for the success of PBEE in any case.

- Estimation of the actual seismic demands on the structural and nonstructural responses can be possible, but only through the application of the provision of seismic

hazard curves for all structures. Also, guides to the input ground motions that are used for the linear and nonlinear analyses should also be provided.

- A database of the existing structures regarding design, construction, and maintenance should be established. Moreover, a database of the mathematical behavior models and the resistance capacity for all kinds of major structural and nonstructural elements should be set up with their probability distributions.
- The linear and nonlinear behavioral models of elements and joints should be verified through experiments, and the reliability in the prediction of the overall structural behaviors using these models should be confirmed. Also, the user of nonlinear software should have a full understanding of the nonlinear analysis and the limitations of the used software.
- A database should be set up for the derivation of the fragility curves of the structural and nonstructural elements and also for the estimation of the economic losses that are due to damages.
- To ensure the true realization of PBEE, the inspection process regarding the quality of the design, construction, and maintenance should be established. For this purpose, a reliable peer-review system should be established and provided.

## 6.2 Conclusions

PBEE can be used as a tool to evaluate the appropriateness of the existing seismic code, which was developed mainly for the high-seismicity regions, and for the adaptation of this code to the lower-seismicity regions. To do this, structures must be designed according to the requirements of the current codes first. Second, perform first- and second-generation PBEE on these designed structures. For example, each building structure (masonry-infilled or masonry structure, RC moment frame, steel moment frame, wall structure, dual structure, and so on) is designed exactly according to the current prescriptive seismic codes, and then they are evaluated using the PBEE procedure. Based on these results, the appropriateness of the performance factors such as the  $R$ ,  $C_d$ , and  $\Omega$  can be verified in terms of the actual behaviors using the PBEE procedure. Also, the maximum deformations in the lower-seismicity regions are estimated with the probability distribution and are used to determine the appropriate requirements for the seismic details, which will clearly lead to the alleviation of the seismic-detail requirements that are intended mainly for high-seismicity regions.

Since any building structure retains some minimum level of earthquake-resistant capacity, it is a sound approach to evaluate this level of resistance and to use this information for the seismic strengthening regarding the targeted maximum earthquake. Though there have been almost no severe earthquake disaster over the past several centuries in Korea, the news of devastated cities around the world due to severe earthquakes might cause unjustified fears among the Korean people and lead to excessive or unnecessary design and construction choices, which should be avoided anyway.

Also, the subjecting of low-rise and high-frequency structures to a very high impulsive or implosive earthquake load that is due to a near-source earthquake can lead to the

brittle-shear failure of the critical beams and columns. Special design requirements to ensure safety against this failure should be developed. The ductility requirement for severe-seismicity regions, however, can be relieved in moderate-seismicity regions.

Although the probability of the collapse of building structures appears to be very low in lower-seismicity regions, the failure of windows, dislocation of ceilings and falling of roof tiles were shown to be highly probable. Since a major portion of the economic loss is due to these non-structural failures, it is necessary to develop appropriate design requirements specific to lower-seismicity regions.

The DE level in the KBC 2016 is similar to that of the IBC 2005 in Sacramento, California, U.S. The South Korean hazard levels of 0.11 and 0.22 g for the earthquakes of the return periods of 500 years and 2400 years in the KBC 2016 are four times larger than the background PGA levels of 0.025 and 0.054 g that have been derived using the approaches of Frankel (1995) and Lam *et al.* (2016). The DE seismic-load level of the KBC 2016 matches the 1940 El Centro ( $M_w=6.9$ ,  $R_{rup}=13$  km) and the 1952 Taft ( $M_w=7.3$ ,  $R_{rup}=43$  km) earthquake levels. The seismic load in South Korea should be reexamined based on the seismological characteristic of the Korean Peninsula, because the current design spectrum does not account for the characteristics of a high acceleration at the high frequencies and a low displacement at the low frequencies.

Deformation ranges of major structures in Korea appear to be just beyond the first significant yielding of the whole structure under MCE in Korea. The characteristics of short durations and low spectral displacement of earthquake records in Korea, and the deformation range of building structures of 0.5% under MCE can lead to the significant alleviation of the strict requirements concerning details for ductility in lower seismicity regions.

## Acknowledgments

The research presented herein was supported by the National Research Foundation of Korea (NRF-2009-0078771), the Ministry of Land, Infrastructure and Transport of Korea (17AUDP-B066083-05), the Ministry of Public Safety and Security of Korea (MPSS-NH-2013-70), and the Korea University Grant. The authors are grateful for the supports of these bodies.

## References

- ACI Committee 318 (2005), Building Code Requirements for Structural Concrete and Commentary (ACI 318-05), American Concrete Institute, Detroit.
- AIK (2000), AIK 2000, Architectural Institute of Korea (AIK), Seoul, Korea. (in Korean)
- AIK (2005), Korean Building Code, KBC 2005, Seoul, Korea. (In Korean)
- AIK (2009), Korean Building Code, KBC 2009, Seoul, Korea. (In Korean)
- AIK (2016), Korean Building Code, KBC 2016, Seoul, Korea. (In Korean)
- ASCE (2010), Minimum Design Loads for Buildings and other Structures, ASCE/SEI 7-10, American Society of Civil

- Engineers (ASCE), Reston, Virginia, US.
- ASCE (2013), Seismic Evaluation and Retrofit of Existing Buildings, ASCE 41-13, American Society of Civil Engineers (ASCE), Reston, Virginia, US.
- ATC (1996a), Improved Seismic Design Criteria for California Bridges: Provisional Recommendations: ATC-32, National Bureau of Standards, Washington DC.
- ATC (1996b), Seismic Evaluation and Retrofit of Existing Concrete Buildings, ATC-40, Applied Technology Council (ATC), Redwood City, CA.
- Atkinson, G.M. (2004), "An overview of developments in seismic hazard analysis", *Proceedings of the 13th World Conference on Earthquake Engineering*, Paper No. 5001.
- Bakun, W.H. and Hopper, M.G. (2004), "Magnitudes and locations of the 1811-1812 New Madrid, Missouri and the 1886 Charleston, South Carolina, earthquakes", *Bull. Seismol. Soc. Am.*, **94**(1), 64-75.
- Boore, D.M. and Atkinson, G.M. (2008), "Ground-motion prediction equations for the average horizontal component of PGA, PGV, and 5%-Damped PSA at spectral periods between 0.01 s and 10.0 s", *Earthq. Spectra*, **24**(1), 99-138.
- Boore, D.M., Campbell, K.W. and Atkinson, G.M. (2010), "Determination of stress parameters for eight well-recorded earthquakes in eastern North America", *Bull. Seismol. Soc. Am.*, **100**(4), 1632-1645.
- Chapman, M.C., Beale, J.N., Hardy, A.C. and Wu, Q. (2016), "Modern seismicity and the fault responsible for the 1886 Charleston, South Carolina, earthquake", *Bull. Seismol. Soc. Am.*, **106**(2), 364-372.
- Chung, K.R., Chung, H.J., Kang, M.S., Kim, S.H. and Park, K.M. (2013), "Eliminating special seismic boundary of special shear wall system using NLTHA", *Korea Concrete Institute Conference*, 2013 Fall, Sokcho, Korea. (in Korean)
- Cornell, C.A. (1968), "Engineering seismic risk analysis", *Bull. Seismol. Soc. Am.*, **58**(5), 1583-1606.
- Cornell, C.A., Jalayer, F., Hamburger, R.O. and Foutch, D.A. (2002), "Probabilistic basis for 2000 sac federal emergency management agency steel moment frame guidelines", *J. Struct. Eng.*, **128**(4), 526-533.
- Fardis, M.N. (2014), Comments on the Seismic Design Provisions of the Korean Building Code 2009. (Opinion Paper)
- FEMA (1996), NEHRP Guidelines for the Seismic Rehabilitation of Buildings, FEMA 273 Commentary, Federal Emergency Management Agency (FEMA), Washington DC.
- FEMA (2000a), Recommended Seismic Design Criteria for New Steel Moment-frame Buildings, Report No. FEMA-350, Washington, DC.
- FEMA (2000b), Prestandard and Commentary for the Seismic Rehabilitation of Buildings, Report No. FEMA-356, Washington, DC.
- FEMA (2012), Seismic Performance Assessment of Buildings, Report FEMA P-58, Federal Emergency Management Agency, Washington DC, U.S.A.
- Frankel, A. (1995), "Mapping seismic hazard in the central and eastern United States", *Seismol. Res. Lett.*, **66**(4), 8-21.
- Günay, S. and Mosalam, K.M. (2013), "PEER performance-based earthquake engineering methodology, revisited", *J. Earthq. Eng.*, **17**(6), 829-858.
- Hong, T.K., Lee, J.H., Kim, W.H., Hahm, I.K., Woo, N.C. and Park, S.J. (2017), "The 12 September 2016 ML 5.8 midcrustal earthquake in the Korean Peninsula and its seismic implications", *Geophys. Res. Lett.*, **44**(7), 3131-3138.
- Houng, S.E. and Hong, T.K. (2013), "Probabilistic analysis of the Korean historical earthquake records", *Bull. Seismol. Soc. Am.*, **103**(5), 2782-2796.
- Hwang, K.R. and Lee, H.S. (2015), "Seismic performance of a 10-story RC box-type wall building structure", *Earthq. Struct.*, **9**(6), 1193-1219.
- ICC (2000), International Building Code, IBC 2000, International Code Council, Country Club Hills, IL.
- ICC (2006), International Building Code, IBC 2006, International Code Council, Country Club Hills, IL.
- Jeong, K.H. and Lee, H.S. (2018), "Ground-motion prediction equation for South Korea based on recent earthquake records", *Earthq. Struct.*, **15**(1), 29-44.
- Ji, J., Elnashai, A.S. and Kuchma, D.A. (2009), "Seismic fragility relationships of reinforced concrete high-rise buildings", *Struct. Des. Tall Spec. Build.*, **18**(3), 259-277.
- Johnston, A.C. (1996), "Seismic moment assessment of earthquakes in stable continental regions-III. New Madrid 1811-1812, Charleston 1886 and Lisbon 1755", *Geophys. J. Int.*, **126**(2), 314-344.
- Korea Meteorological Administration (KMA), <http://www.kma.go.kr/>. (in Korean)
- Korean Broadcasting System (KBS), <http://news.kbs.co.kr/news/view.do?ncd=3366101>. (in Korean)
- Kramer, S.L. (1996), *Geotechnical Earthquake Engineering*, Prentice Hall, New York.
- Krawinkler, H. and Miranda, E. (2004), *Performance-based Earthquake Engineering, Chapter 9 of Earthquake Engineering: from Engineering Seismology to Performance-based Engineering*, Eds. Bozorgnia and V.V. Bertero, CRC Pres.
- Lam, N., Tsang, H., Lumantarna, E. and Wilson, J. (2016), "Minimum loading requirements for areas of low seismicity", *Earthq. Struct.*, **11**(4) 539-561.
- LATBSDC (2017), An Alternative Procedure for Seismic Analysis and Design of Tall Buildings Located in the Los Angeles Region, Los Angeles Tall Buildings Structural Design Council, A consensus Consensus Document, June.
- Lee, C.H. (2017), "Earthquake engineering analysis of ground accelerations measured in the 912 Gyeong-ju earthquake", *J. Koran Soc. Civil Eng.*, **65**(4), 8-13. (in Korean)
- Lee, H.S. and Woo, S.W. (2002a), "Seismic performance of a 3-story RC frame in a low-seismicity region", *Eng. Struct.*, **24**(6), 719-734.
- Lee, H.S. and Woo, S.W. (2002b), "Effect of masonry infills on seismic performance of a 3-storey R/C frame with non-seismic detailing", *Earthq. Eng. Struct. Dyn.*, **31**(2), 353-378.
- Lee, H.S., Hwang, K.R. and Kim, Y.H. (2015), "Seismic performance of a 1: 15-scale 25-story RC flat-plate core-wall building model", *Earthq. Eng. Struct. Dyn.*, **44**(6), 929-953.
- Lee, H.S., Hwang, S.J., Lee, K.B., Kang, C.B., Lee, S.H. and Oh, S.H. (2012), "Earthquake simulation tests on a 1: 5 scale 10-story RC residential building model", *The 15th World Conference on Earthquake Engineering (15WCEE)*, Lisbon, Portugal.
- McGuire, R. (1976), "Probabilistic seismic hazard analysis and design earthquakes: closing the loop", *Bull. Seismol. Soc. Am.*, **85**(5), 1275-1284.
- Moehle, J. and Deierlein, G.G. (2004), "A framework methodology for performance-based earthquake engineering", *The 13th World Conference on Earthquake Engineering*, Paper No. 679, August, Vancouver, B.C., Canada.
- NEMA (2012), Active Fault Map and Seismic Hazard Map, National Emergency Management Agency, Report No. NEMA-NH-2009-24. (in Korean)
- Nordenson, G.J. and Bell, G.R. (2000), "Seismic design requirements for regions of moderate seismicity", *Earthq. Spectra*, **16**(1), 205-225.
- Nuttl, O.W., Bollinger, G.A. and Herrmann, R.B. (1986), "The 1886 Charleston, South Carolina, earthquake; a 1986 perspective, US Geological Survey circular 985, USGS, Denver.
- Ohmynews [http://www.ohmynews.com/NWS\\_Web/View/at\\_pg.aspx?CNTN\\_CD=A0002243576](http://www.ohmynews.com/NWS_Web/View/at_pg.aspx?CNTN_CD=A0002243576). (in

- Korean)
- Porter, K.A. (2003), "An overview of PEER's performance-based earthquake engineering methodology", *Proceedings of 9th International Conference on Applications of Statistics and Probability in Civil Engineering*.
- Scholz, C.H. (2002), *The Mechanics of Earthquakes and Faulting*, Cambridge University Press.
- SEAOC (1995), *Vision 2000, Performance Based Seismic Engineering of Buildings, Vols. I and II: Conceptual Framework*, Structural Engineers Association of California (SEAOC), Sacramento, CA.
- SEAONC (2007), Requirements and Guidelines for the Seismic Design and Review of New Tall Buildings Using Non-Prescriptive Seismic Design Procedures, AB-083: Guidelines for the Structural Review of New Tall Buildings, Structural Engineering Association of Northern California.
- Tall Buildings Initiative. TBI (2010), Guidelines for Performance-Based Seismic Design of Tall Buildings, Pacific Earthquake Engineering Research Center.
- USGS <https://earthquake.usgs.gov/earthquakes/eventpage/us20005iis#finite-fault>. (in Korean)
- Willford, M., Whittaker, A. and Klemencic, R. (2008), *Recommendations for the Seismic Design of High-rise Buildings*.
- Yonhapnews <http://www.yonhapnews.co.kr/bulletin/2016/09/19/0200000000AKR20160919070351053.html>. (in Korean)
- YTN [http://www.ytn.co.kr/\\_ln/0115\\_201609131800184070](http://www.ytn.co.kr/_ln/0115_201609131800184070). (in Korean)